SEASONAL VARIATION OF SURFACE ENERGY FLUXES ABOVE A MIXED SPECIES AND SPATIALLY HOMOGENEOUS GRASSLAND

by

NICHOLAS C. MOYO

B.Sc. Hons. (Environmental Science), University of KwaZulu-Natal

Thesis submitted in fulfilment of the academic requirements for the degree of

MASTER OF SCIENCE

in Agrometeorology

Soil-Plant-Atmosphere-Continuum Research Unit

School of Environmental Sciences

Faculty of Science and Agriculture

University of KwaZulu-Natal

Pietermaritzburg

South Africa

September, 2011

Declaration

I hereby declare that the research work reported in this dissertation is the result of my own original investigations except where acknowledged. It has not been submitted for any degree or examination at any other university.

Candidate: Nicholas C. Moyo

Signed ………………………

Date …………………………

Supervisor: Michael J. Savage

Senior Professor of Agrometeorology

Signed ………………………..

Date …………………………..

Acknowledgements

I wish to thank my supervisor Professor Michael J. Savage for his insightful comments, invaluable help and patience throughout the course of the study. I am also grateful to Mrs Jothimala Manickum for administrative work and moral support, Dr Michael Abraha and Dr Eltayeb Nile for the diversified help during field and laboratory work.

Funding from the Agrometeorology Discipline, University of KwaZulu-Natal, for this study is gratefully acknowledged. My thanks also go to Mr Craig Morris for allowing me to conduct my trial at the Grassland Research Site, Ukulinga Research Farm, Pietermaritzburg, South Africa. I also thank Mr Jerry Naiken (Grassland Science) for the technical support and assistance during the preparation on treatment plots. The use of equipment, purchased using Water Research Commission funds is acknowledged (projects K349, K1335 and K1567) and much appreciated. The funds for the four-component net radiometer were provided by an expensive capital equipment grant from the UKZN Research Office. The Electronics Centre is acknowledged for their assistance in the trouble-shooting of equipment.

I would like to express my special thanks to my parents and the rest of the family for their endless support and patience during my long absence from them. My sincere thanks also go to all my friends for their continuous encouragement and moral support during my study period.

Finally, I would like to thank my Creator and heavenly Father for His endless guidance, grace and love shown to me during my studies.

Abstract

The increasing human population, industrialization, urbanisation and climate change challenges have resulted in an increased demand for already scarce water resources. This has left the agricultural sector with less water for production. Sustainable water management strategies would therefore require accurate determination of water-use. In agriculture, water-use can best be determined from total evaporation which is the loss of water from soil and vegetation to the atmosphere. Accurate quantification of total evaporation from vegetation would require a thorough understanding of water transport processes between vegetation and the atmosphere, especially in a water-scarce country like South Africa.

Several methods for estimating total evaporation have been developed and are in use today. Some of the common methods used today are: the Bowen ratio energy balance, eddy covariance, scintillometry, flux variance and surface renewal. However, various methods have advantages and disadvantages. Considerations include the cost of equipment and level of skill required for use of some of the methods. A number of methods involve indirect or direct estimation of sensible heat flux then calculating latent energy flux and hence total evaporation as a residual of the shortened energy balance equation. The main objective of this study is to determine the effects of grassland management practices on the energy balance components as well as on the surface radiation balance.

Eddy covariance and surface renewal methods were employed to investigate the effects of grassland management practices (mowing and burning) on the micrometeorology of naturally occurring grassland. A 4.5-ha grassland site (Ukulinga, Pietermaritzburg, South Africa) was divided into two halves: one area was initially mowed (cut-grass site) to a height of 0.1 m

while the other was not mowed (tall-grass site). The tall-grass site was later treated by burning and hence referred to as the burnt-grass site. Two eddy covariance systems were deployed, one at each of the cut-grass and the tall-grass sites. The systems each comprised a three-dimensional sonic anemometer to measure high frequency sonic temperature, orthogonal wind speeds and directions and the eddy covariance sensible heat flux (W m^{-2}). Latent energy flux, from which total evaporation was then determined, was calculated as a residual from the shortened energy balance equation from measurements of sensible heat flux, net irradiance and soil heat flux assuming closure is met.

Other microclimatic measurements of soil water content, soil temperature, surface reflection coefficient and reflected solar irradiance were performed, the latter with a four-component net radiometer. An automatic weather station was also set up at the research site for continuous measurements of solar irradiance, air temperature, relative humidity, wind speed and direction and rainfall. Water vapour pressure and grass reference evaporation were also determined online.

Energy fluxes from the tall-grass site were measured from March to June 2008. Greater total evaporation rates (2.27 mm day^{-1}) were observed at the beginning of the experiment (March). As winter approached most of the energy balance components showed a constant decreasing trend and the average total evaporation rates for May and June were 1.03 and 0.62 mm day^{-1}, respectively.

The tall-grass site had consistently lower soil temperatures that changed diurnally when compared to the cut-grass site. The soil water content at both sites showed no significant differences. Most of the energy balance components were similar between the two sites and changed diurnally. Although there were small differences observed between other energy balance components, for example, latent energy flux was slightly greater for the tall-grass site than for the cut-grass site. The tall-grass site had more basal cover and this may have contributed to the differences in temperature regimes observed between the two sites. However, the plants growing at the cut-grass site showed more vigour than the ones at the tall-grass site as spring approached.

Burning of a mixed grassland surface caused significant changes to most of the optical properties and energy fluxes of the surface. Following burning, the soil temperature was elevated to noticeable levels due to removal of basal cover by burning. The surface reflection coefficient measured before and after the burn also presented a remarkable change. The surface reflection coefficient was significantly reduced after the burn but a progressive increase was observed as the burnt grass recovered after the spell of spring rains. The energy fluxes: net irradiance, latent energy flux and soil heat flux also increased following the burn but the latent energy flux was reduced as transpiration was effectively eliminated by the burning of all actively transpiring leaves. As a result, the main process that contributed towards latent energy flux was soil evaporation.

An ideal surface renewal analysis model based on two air temperature structure functions was used to estimate sensible heat flux over natural grassland treated by mowing. Two air temperature lag times r (0.4 and 0.8 s) were used when computing the air temperature structure functions online. The surface renewal sensible heat fluxes were computed using an iteration process in Excel. The fluxes, obtained using an iterative procedure, were calibrated to determine the surface renewal weighting factor (α) and then validated against the eddy covariance method using different data sets for unstable conditions during 2008. The latent energy flux was computed as a residual from the shortened energy balance equation. The surface renewal weighting factor was determined for each of the two heights and two lag times for each measurement height (z) above the soil surface. The α values obtained during the surface renewal calibration period (day of year 223 to 242, 2008) ranged from 1.90 to 2.26 for measurement height 0.7 m and r = 0.4 and 0.8 s. For a measurement height of 1.2 m and r = 0.4 and 0.8 s, α values of 0.71 and 1.01 were obtained, respectively. Good agreement between surface renewal sensible heat flux and eddy covariance sensible heat flux was obtained at a height of 1.2 m using α = 0.71 and a lag time of 0.4 s.

Total evaporation for the surface renewal method was compared against the eddy covariance method. The surface renewal method, for a height of 1.2 m and a lag time of 0.4 s, yielded 1.67 mm while the eddy covariance method yielded 1.57 mm for a typical cloudless day. For the same day for a measurement height of 1.2 m and a lag time of 0.8 s, eddy covariance and surface renewal methods yielded 1.57 and 1.10 mm, respectively. For a lag time of 0.4 s, the surface renewal method overestimated total evaporation by 0.10 mm while for a lag time of 0.8 s, the total evaporation was underestimated by 0.47 mm. As a result, the surface renewal method performed better for z = 1.2 m and a lag time of 0.4 s. The eddy covariance method gave reliable sensible heat fluxes throughout the experiment and this allowed a comparison of fluxes across all treatment areas to be achieved. The short-term analysis of the surface renewal method also gave reliable energy fluxes after calibration. Compared to the eddy covariance method, the surface renewal method is more attractive in the sense that it is easy to operate and use and it is relatively cheap. However, the surface renewal method requires calibration and validation against a standard method such as the eddy covariance method.

This study showed that grassland management practices had a considerable effect on surface radiation and energy balance of the mowed and burnt treatment sites. Total evaporation was mainly controlled by the available energy flux, rainfall and grassland surface structure. High total evaporation values were observed during summer when net irradiance was at its highest and grass growth at its peak. Low total evaporation values were observed in winter (dry atmospheric conditions) when net irradiance was at its lowest and most vegetation was dormant.

Table of contents

List of figures

List of tables

Chapter 1: Introduction

1.1 Motivation and objectives

Escalating human population, industrialization, urbanisation and climate change challenges have resulted in competition for fresh water between the various water-use sectors, including agriculture. Population growth, urbanisation and industrialization have compromised food production to sustain life, timber production to provide infrastructure, fodder production to sustain livestock and water reticulation systems to increase access to clean water and sustain waste treatment operations. Fresh water, a scarce resource, shared by almost all humanity, including agricultural and industrial sectors has prompted decision makers to suggest monitoring water usage and charging for these (Postel, 2000; United Nations, 2009a, b).

South Africa, already classified as a semi-arid country, is no exception from the rest of African nations facing water scarcity (Falkenmark, 1989; Falkenmark, 1990; Department of Environmental Affairs and Tourism, 2006). The pressing issues of water resources depletion led to the implementation of the 1998 South Africa National Water Act which refers to the charging and equitable allocation of fresh water and recognizing detrimental activities that may result in streamflow reduction. Sustainable water management strategies are therefore required to meet the ever-increasing demands on water resources. In order to monitor water resources, it is vital to understand the hydrological cycle especially the evaporation and transpiration components (Savage *et al*., 1997; Savage *et al*., 2000; Savage *et al*., 2004). The quantification of water loss from agricultural crops, grasslands, commercial plantations, open water and other surfaces requires multidisciplinary expert knowledge thereby requiring a holistic approach from all stakeholders to combat water problems.

The role of grasslands in the agricultural and wildlife sectors is important as they are the main providers of food to a variety of domesticated and wild animals. The role of grassland communities as primary producers cannot be overlooked but also serve as an active surface influencing energy balances of the land surface on a large scale (Rosset *et al*., 1997), thereby are impacting significantly on climate change. A number of factors may influence radiation and energy balances of a land surface, for instance, the diurnal and seasonal weather variations due to the Earth's revolution around its own axis and rotation around the sun, respectively. Some studies have shown that most radiation and energy balance components peak at noon with minimums occurring at sunrise and sunset (Savage, 1980; Savage and Vermeulen, 1983; Bremer and Ham, 1997). Grassland management practices greatly modify grassland surfaces, thereby indirectly impacting surface radiation and energy balance (Wang and Davidson, 2007) at both the seasonal and diurnal time scales. Radiation and energy balances of grassland communities, subjected to various management practices, have been the focus of a number of investigations (Savage and Vermeulen, 1983; Bremer and Ham, 1999; Twine *et al*., 2000; Watts *et al*., 2000; Everson, 2001; Hunt *et al*., 2002; Baldocchi *et al*., 2004; Falge *et al*., 2005; Odhiambo, 2007; Jacobs *et al*., 2008; Mengistu, 2008; Moran *et al*., 2009).

Grassland management practices include: mowing, burning, fertilization, the grazing animal (Dillon, 1980; Wright and Bailey, 1982; Harrington *et al*., 1984; Pearson and Ison, 1997) and irrigation (Edwards and Tainton, 1990). These management practices have been reported to influence grassland structural canopy development, thereby affecting radiation balances and the partitioning of available energy fluxes. It is, therefore, important to understand atmospheric dynamics and various components of surface radiation and energy balance above different grassland surfaces (Rosset *et al*., 1997). These fluxes may be obtained using different micrometeorological methods such as eddy covariance (EC), flux variance (FV), surface layer scintillometry (SLS), surface renewal (SR), Penman-Monteith method, Bowen ratio energy balance (BREB) methods and lysimetry (Rosset *et al*., 1997; Gavin *et al*., 2000; Castellví *et al*., 2008; Mengistu, 2008; Odhiambo, 2008; Abraha, 2010; Castellví and Snyder, 2010; Savage, 2010b; Mengistu and Savage, 2010a,b).

The EC method is regarded as a standard method for direct and point measurement of sensible heat and latent energy flux (W m^{-2}) (Mauder *et al*., 2007). This method uses high frequency, typically 10 Hz, air temperature and water vapour pressure measurements. The SLS method involves fluctuation intensity measurements of visible or infrared radiation after propagation. These optical measurements may be achieved with a scintillometer and measures refractive index fluctuations, over atmospheric path lengths from 50 up to 300 m, from which H may be computed (Savage *et al*., 2004).

Surface renewal is a relatively new and simpler method for estimating sensible heat flux and has been tested successfully over mixed community grassland (Savage *et al*., 2004), kikuyu grass (Mengistu, 2008), maize, orchard and forest canopies (Paw U *et al*., 1995). In comparison to the EC method, the SR method is also a high frequency method but uses a single-temperature measurement, from which H is calculated.

The BREB method is a method traditionally used for estimating evaporation. This method uses profile difference measurements of air temperature and water vapour pressure. Surface net irradiance and soil heat flux measurements are also required. There have been only a few investigations using micrometeorological methods above treated (mowed, burnt, fertilized and/or irrigated) grass surfaces. As a result, more research is required to test such methods above grassland communities to test their performance and to quantify the rate of total evaporation from grassland communities. In this study, both the EC and SR methods will be used to estimate sensible heat flux above mowed, burnt and undisturbed grassland surfaces. Turbulence fluxes obtained from SR method will be used only for comparison purposes. Total evaporation above different grassland surfaces will be estimated as a residual of the shortened energy balance equation using measured sensible heat flux and other measurements of net irradiance and soil heat flux. The components of the surface radiation balance will be obtained using a four-component net radiometer.

1.2 Aims and objectives

The aims of this study were to quantify the spatial and temporal patterns of radiation and energy balance components above different grassland surfaces (tall, mowed and burnt grass) using EC and SR methods. The objectives of this study were to determine the effects of grass mowing and burning on the energy balance components as well as on the radiation balance.

1.3 Thesis structure

Chapter 1 introduces the study, giving an overview of some of the micrometeorological methods that have been successfully used to estimate energy balance of land surfaces, especially grasslands.

Chapter 2 focuses on the theoretical background of some of the micrometeorological methods used in this investigation, emphasising the application of such methods above grassland surfaces.

Chapter 3 focuses on tall grassland energy balances. A detailed description of the materials and methods is presented. The EC method, used to obtain sensible heat flux above a natural tall grass surface, is discussed in detail. Evaporation is calculated as a residual of the shortened energy balance. Measurements and comparison of other energy balance components are also presented.

Chapter 4, an experimental chapter, focuses on the influence of mowing on the energy balance of tall grassland.

Chapter 5 investigates the influence of burning on radiation and energy balances of tall grassland. Influences of burning on the surface reflection coefficient and evaporation estimation are also discussed, as in Chapters 3 and 4.

Chapter 6 focuses mainly on the application of SR method. The theory of the SR method for estimating the sensible heat flux will be elaborated in detail.

Chapter 7 is a summary of the conclusions and recommendations for future study.

Chapter 2: Literature review

Total evaporation plays a vital role in the hydrological cycle. Precipitation over oceans, ice, rock and many other different surface types is returned into the atmosphere as water vapour. Penman (1948) defined various surfaces from which evaporation occurs: "vegetation, on which plant leaves act as transpiring surfaces; bare or fallow soil, from which water evaporates at, or just below, the soil-air interface and open water, from which evaporation takes place directly". These evaporating surfaces are equally important but this study focuses on grassland surfaces only. Grasslands cover significant areas (Rosset *et al*., 1997) which influence radiation and energy balances of land surfaces on a large scale and subsequently impact on the hydrological cycle.

The energy balance of commercial grasses, such as sugarcane, sorghum and maize, as opposed to naturally occurring grass species have previously been studied (Hurtalová and Matejka, 1999; Zapata and Martínez-Cob, 2002; Castellvi *et al*., 2006; Nile, 2010). Naturally occurring grasslands are more abundant than commercial grasslands, justifying the research on energy balance of naturally occurring grassland communities. Locally, several studies have been carried out on montane grassland using micrometeorological techniques (Savage *et al*., 1997, Savage *et al*., 2009) and more recently in a mesic grassland in the eastern part of South Africa (Savage *et al*., 2010). Selected radiation laws, energy balance components and various methods for measuring sensible heat flux are presented.

2.1 Measurement of radiation

Solar irradiance is a significant contributor to net irradiance, the most vital component of energy balance equation. It is responsible for driving evaporation, a hydrological component and the processes of air and soil surface heating (Everson *et al.*, 1998). The main energy source driving all life supporting processes is the sun. In addition to evaporation, other important processes are transpiration and photosynthesis. "The most important process responsible for energy transfer in the atmosphere is the electromagnetic radiation" (Liou, 2002).

Radiation may be divided into several components. Short-wave or solar irradiance consists of wavelengths from 280 nm to 2800 nm whilst infrared irradiance ranges from 2800 to 100 000 nm. Infrared irradiance is mainly affected by the greenhouse gases, especially water vapour and carbon dioxide present in the atmosphere (Bugbee and Klassen, 2005).

Solar irradiance is spatially and temporally variable but is constant at the top of the Earth's atmosphere with a value of 1370 W m^{-2}, usually termed as solar constant (Bugbee and Klassen, 2005). Solar irradiance can be divided into direct and diffuse components. On average, for cloudless skies, a solar irradiance of 900 to 1000 W m^{-2} reaches the Earth's surface with the remainder being scattered or absorbed by water vapour, carbon dioxide, ozone, and/or particulates in the atmosphere (Bugbee and Klassen, 2005).

2.2 Blackbody radiation laws

The term "blackbody" refers to a material that completely absorbs incident radiation. Radiation emission by a blackbody is the opposite of absorption. Radiation emitted by a surface is repeatedly reflected and re-absorbed by the surface. Thus, the radiation is weakened by the absorption and strengthened by the new emission. Emission and absorption repetitions will then reach equilibrium with respect to the surface temperature of the material (Liou, 2002). Some of the fundamental laws governing blackbody radiation are: Planck's Law and Stefan-Boltzmann Law.

2.2.1 Planck's Law

Planck assumed that atoms that make up a material behave like electromagnetic oscillators, each having a characteristic frequency of oscillation. The oscillators emit energy into the material and absorb energy from it. Planck first proposed that an oscillator can only have energy given by:

$$E = nh\upsilon \tag{2.1}$$

where n is quantum number and can take only integral values, h Planck's constant and v the oscillator frequency. Equation (2.1) asserts that the oscillator energy is quantized through the quantum number n. Secondly, Planck postulated that the oscillators do not emit energy continuously, but only quanta. These quanta of energy are emitted when an oscillator changes from one to another of its quantized energy states. As a result, if the quantum number changes by one unit, the change in the amount of radiated energy is given by:

$$\Delta E = \Delta n\, h\upsilon = h\upsilon \qquad (2.2)$$

Determination of the emitted energy requires knowing the total number of oscillators with frequency υ for all possible states. Following the preceding postulations and normalization of the average emitted energy per oscillator, the Planck function $B_{\upsilon}(T)$ expresses the energy per unit area per unit time interval per unit steradian (1 steradian = m^2 m^{-2}) per unit frequency interval given by:

$$B_{\upsilon}(T) = \frac{2h\upsilon^3}{c^2\left(e^{h\upsilon/KT} - 1\right)} \qquad (2.3)$$

where c is the speed of light, K Boltzmann's constant and T the absolute temperature. According to Liou (2002), the Planck and Boltzmann constants have been determined through experimentation and are h = 6.626 x 10^{-34} J s and K = 1.3806 x 10^{-23} J K^{-1}, respectively.

2.2.2 Stefan-Boltzmann Law

The broadband flux is the total energy over all wavelengths (F, W m^{-2}):

$$F = \int_0^{\infty} B_{\lambda}\, d\lambda \qquad (2.4)$$

where B_λ is the amount of energy per unit area per unit time per unit steradian at a given wavelength λ. The integration in Eq. (2.4) yields Stefan-Boltzmann relationship, the total flux (W m^{-2}) from a blackbody at temperature T (K):

$$F = \sigma T^4 \tag{2.5}$$

where σ is Stefan-Boltzmann's constant equal to 5.6704 x 10^{-8} W m^{-2} K^{-4}. Equation (2.5) gives the total flux from a so-called "blackbody" or "perfect radiator" at the emittance temperature *T*. It has been noted that in reality, most terrestrial surfaces are "grey bodies" in the thermal infrared, meaning that the emitted radiation is nearer to, but somewhat less than that from a perfect emitter, or radiator. To account for this, a scaling constant was introduced, called the "emissivity" (ε, dimensionless), defined as a ratio of the actual flux from a grey body to that of a perfect emitter at the same temperature. Emissivity is a characteristic of the material surface and often the frequency of emission from the material. Hence different materials bear different emissivities (Campbell and Diak, 2005). The emittance *F* (W m^{-2}) from a grey body is given by:

$$F = \varepsilon \sigma T^4 \tag{2.6}$$

In Eq. (2.6), ε is the emissivity of the surface for the whole wavelength range.

2.3 Surface radiation and energy balance exchange

Two energy flux components at the Earth's surface are the sensible heat flux *H* and the latent energy flux *LE*. *H* results in temperature change with no phase change of water while *LE* results in a phase change of water most commonly from liquid to vapour at a constant temperature or almost no temperature change. The ratio H/LE is important because it is used for partitioning the energy balance into its various terms. This ratio is referred to as the Bowen ratio β.

2.4 Net irradiance

Net irradiance measurements are crucial for most micrometeorological applications. Net irradiance components are determined by suspending an instrument, or set of instruments, above a surface of interest to cause minimal disturbance to the surface radiation balance. Most radiation components may be obtained using the Kipp and Zonen CNR1 four-component net radiometer. This instrument gives the most set of information and consists of five sensors, one pair facing up and down for irradiance measurements. There is also an internal temperature sensor for computing the infrared irradiance from the top surface of the instrument to the atmosphere and the infrared irradiance from the bottom surface. The irradiance sensors have filters limiting wavelengths of radiation to which they will respond. For instance, pyranometers are sensitive only to solar irradiance while pyrgeometers respond only to infrared irradiance (Campbell and Diak, 2005). The net irradiance R_n for a flat extensive surface is computed as the difference between up-facing and down-facing pairs:

$$R_n = I_s - r\,I_s + L_d - L_{\mathrm{u}} \tag{2.7}$$

where I_s represents the incoming solar irradiance, rI_s the reflected solar irradiance and L_d and L_u are the downward and outgoing infrared irradiances, respectively. Reflected solar irradiance has a significant role, via R_n, in the energy budget equations used to estimate environmental quantities like total evaporation, sensible heat flux, soil heat storage, photosynthesis and other environmental factors. One of the applications of surface reflection coefficient r is in air pollution models where values are required as an input to determine photochemical rates in the atmosphere (Idso, 1976; Angle *et al.*, 1992). Also, with increased global warming, the reflection of iced and snowed regions of the world is decreasing, resulting in increased absorption of solar irradiance and more melting. This mechanism is referred to as the Arctic amplification (Graversen and Wang, 2009; Serreze *et al.*, 2009; Inoue and Hori, 2011).

The surface reflection coefficient is of concern in many scientific applications and changes have directly been linked to human activities, such as agricultural practices, (Arya, 1988). Significant changes in local or regional reflection coefficients may cause significant changes to the partitioning of the surface energy fluxes at the Earth's surface, hence causing modifications to the microclimate. Agricultural practices such as irrigation have lowered surface reflection coefficients of wetted surfaces; these coefficients also show diurnal and seasonal variations. Sunrise times are characterised by large reflection coefficient values while afternoon times have low values (Arya, 1988).

The available energy flux A (W m^{-2}) is the difference between net irradiance and energy flux G stored by the soil (Savage, 1997):

$$A = R_n - G = LE + H + \xi F_c \tag{2.8}$$

The net irradiance R_n (W m^{-2}) minus soil heat flux G (W m^{-2}), at a vegetated surface, is partitioned into sensible H and latent LE energy flux densities, and photosynthetic flux ξF_c where ξ is the quantum yield (J kg^{-1}) and F_c is the flux of carbon dioxide in kg s^{-1} m^{-2}. The shortened energy balance equation neglects advection and photosynthetically stored heat flux densities in the canopy as they are considered negligible yielding:

$$R_n = LE + H + G \qquad (2.9)$$

The sign convention in Eq. (2.9) is that during the day the net irradiance is positive with terms on the right hand side of the shortened energy balance equation leaving the Earth's surface being regarded as positive. The other convention requires that the terms leaving the surface are negative and hence:

$$R_n + LE + H + G = 0 \qquad (2.10)$$

In Eq. (2.10), the sign convention results in negative latent energy and sensible heat values under normal daytime conditions and the reverse happens at night (Savage, 1997).

2.5 Other parameters for energy balance computation

2.5.1 Soil temperature

Temperature is a measure of the thermal energy level of an object and it is one of the most basic quantities that describe the physical state of the soil. The amount of thermal energy gained or lost required to cause a unit change in temperature for a unit mass of the material is defined by its specific heat capacity (the amount of thermal energy needed to increase the temperature of a unit mass by a unit temperature difference) (Fritschen and Gay, 1979). Low or high soil temperature can directly or indirectly affect the functioning of ecosystems, plant development and energy fluxes (Savage, 1980). Soil temperature measurement is, therefore, of paramount importance for various environmental and agricultural applications (Novak, 2005). There are several temperature sensors that can be used to accurately measure soil temperature. Despite a wide range of instrument choice, problems associated with soil temperature measurements have been identified. One of the issues is the placement of the temperature sensors without disturbing the flow of heat in the soil, the structure of the soil and furthermore the soil medium is variable. However, developments of new temperature devices have led to much easier techniques of inserting sensors into the soil profile. The techniques for placing temperature sensors into a soil medium have been described in detail by Fritschen and Gay (1979).

For micrometeorological applications, soil temperature measurements above the soil heat flux plates are required. These measurements are then used to compute the rate of change in soil temperature, dT_{soil} / dt, for a defined soil depth (typically between 20 and 60 mm) (Savage *et al.*, 1997).

2.5.2 Soil water content

Soil water content plays a vital role in understanding soil ecological dynamics, soil fertility, soil microbiology and various micrometeorological applications. Several instruments for measuring soil water regimes have been used and they all have different performances. As in the case for dT_{soil}, the measurement of soil water content θ_w is equally important in understanding the surface energy flux dynamics.

2.5.3 Soil heat flux

The thermal energy that is transported per unit area per unit time is referred to as the soil heat flux G. The calculation of G is important in micrometeorological studies because it couples energy transfer processes at the Earth's surface with the energy transfer processes within the soil medium (Sauer, 2005). Sometimes the term G is neglected since its magnitude is small compared to other energy balance terms. In other cases, the daily and yearly totals of soil heat flux have been found to be close to zero. Nevertheless, daily and sub-daily values have been found to be significant when the soil is heating or cooling diurnally. Fritschen and Gay (1979) have emphasized that omitting soil heat flux measurements from hourly budget analysis will introduce phase errors although the daily sums are relatively unaffected. Soil heat flux can be computed from temperature gradients provided the soil thermal conductivity is known. Alternatively, it can be computed from changes in soil temperature with time if the specific heat capacity of the medium is known. Good estimates of soil heat flux can be obtained using commercially available transducers. The flow of thermal energy through the soil heat flux transducer G_t is related to temperature difference across the transducer:

$$G_t = \frac{\lambda(T_t - T_b)}{l} \tag{2.11}$$

where λ is the thermal conductivity of the transducer, l the thickness of the transducer, and T_t and T_b the temperatures at the top and the bottom of the transducer respectively. The transducer is made up of a thermopile which generates a voltage difference in response to $\Delta T = T_t$ - T_b that is directly proportional to the heat flux across the transducer G_t.

Soil heat flux plates implanted too close to the soil surface, impair energy and mass flow in the soil profile (Fritschen and Gay, 1979). It is therefore recommended to implant them at a typical depth of 80 mm below the soil surface. An additional measurement of temperature using averaging thermocouples is required to estimate the thermal energy flux stored above the plate (G_{stored}). The G_t and the G_{stored} are then summed up to give the total G (Savage *et al.*, 1997):

$$G = G_t + G_{stored} \tag{2.12}$$

where G_{stored} = stored energy/ (area x time) =

$$M_{soil}\, dT_{soil}\, c_{soil} / (At) = \rho_{soil}\, V_{soil}\, dT_{soil}\, c_{soil} / (At) = \rho_{soil}\, \Delta z_{soil}\, dT_{soil}\, c_{soil} / dt \tag{2.13}$$

where ρ_{soil} is the bulk density of the soil, and the soil depth Δz = 0.08 m (depth below the soil surface). The term dT_{soil} is the temporal change in soil temperature above the soil heat flux transducer, $\rho_{soil}\, c_{soil}$ the volumetric heat capacity of the soil and dt the time interval between consecutive datalogger output storage (typically 20 or 30 minutes). The volumetric heat capacity of the soil under study is determined by summing the volumetric heat capacity of the dry soil and specific heat capacity of water:

$$\rho_{soil}\, c_{soil} = \rho_{soil} c_{dsoil} + \rho_w \theta_v c_w \tag{2.14}$$

where $\rho_{soil}\, c_{dsoil}$ is the volumetric heat capacity of the dry soil, θ_v the soil water content (volume basis in m^3 of water per m^3 of soil) and $\rho_w c_w$ = 4190 J m^{-3} $^oC^{-1}$ (volumetric heat capacity of water) where ρ_w is the density of water (Savage *et al*., 1997).

2.6 Methods of evaporation and transpiration estimation

2.6.1 Evaporation

Evaporation is the process by which water is transferred from the land to the atmosphere (the evaporation may take place from the soil and other surfaces). The transformation from liquid water to water vapour involves a change in phase without a change in temperature. The evaporation of water occurs anytime and everywhere in the hydrologic cycle, from precipitation (raindrops and hail), vegetation, land and water surfaces. Evaporation is commonly referred to as a latent process because there is almost no temperature change during the process. Conversely, the part of the heat energy transport which results in a temperature change with no change in phase is referred to as sensible heat. The sun (solar energy) is the main driver of most processes in the hydrologic cycle (Savage *et al*., 1997).

Evaporation is one of the most vital components of the hydrologic cycle. The evaporation process is difficult to quantify and accurate measures of this component are required to make informed decisions in agriculture, mining, and other water use sectors. Micrometeorological research has focused on both short-term and long-term investigations in which water vapour fluxes are measured. The measured fluxes are analysed and compiled to get diurnal and seasonal variations of water loss. The instrumentation used in performing these tasks are often complex. If necessary precautions are not taken during data collection, data collected may be biased leading to large errors in the water and energy budgets calculated. It is, therefore, important to re-examine the methods of flux measurement techniques to ensure the highest data integrity (Meyers, 2005).

2.6.2 Transpiration

Transpiration is a process whereby water vapour is lost from plant leaves through their stomata. The term "total evaporation" *ET* refers to the collective processes of water movement into the atmosphere. *ET* can be partitioned into soil evaporation *E* and transpiration *T* since both occur simultaneously (Jarmain, 2003).

The most commonly used techniques for measurement of transpiration are heat pulse velocity (HPV) and the stem steady state heat energy balance (SSS) techniques (Sakuratani, 1981; Edwards and Warwick, 1984; Smith and Allen, 1996). The heat pulse velocity technique involves measurement of speed of a heat pulse moving through a plant sap. The system consists of a datalogger, power supplies, one heater probe with a thermistor probe above the heater and another below the heater.

The merits of the HPV technique are that it is reliable and inexpensive technique. Its reliability allows for simultaneous measurements of transpiration for many tree stands. The HPV technique also allows for the automation of data collection and storage (Dye *et al*., 1991). The disadvantages of the technique are that the accuracy of the technique is reduced for low sap fluxes. Also, since this technique is intrusive, the sap flux estimates may be sensitive to wound width where the sap flow is interrupted. It is also destructive since tree felling may be necessary to determine corrections for the wound. A detailed description of the HPV technique has been presented by Edwards and Warwick (1984); Dye *et al*. (1991); Smith and Allen (1996); Hall *et al*. (1998) and Köstner *et al*. (1998).

The stem steady state heat energy balance (SSS) technique is based on fundamental theory and requires a continuous constant supply of heat energy flux (J s^{-1}) to a plant steam. The heat energy flux is supplied using a surrounding heater. By accounting for the assumed component energy losses by: (a) conduction both vertically upwards and downwards through and radially from the stem, and (b) heat stored in the plant stem, it is possible to determine the heat component convected in sap. A detailed description and practical application of the SSS technique has been discussed by Sakuratani (1981) and Savage *et al*. (2000).

2.6.3 Reference evaporation

Reference evaporation (ET_o) refers to the total evaporation from a reference surface and is related to the transpiration of different crops by means of a crop factor where the crop has adequate water and nutrients and fully covers the soil surface. Short grass that is not short of water and nutrients and fully covers the surface has been accepted as a reference surface (Allen *et al*., 1998). The reference crop (short grass) also should have a fixed height of 0.12 m, surface reflection coefficient (r) of 0.23 and surface resistance (r_s) of 70 s m^{-1} (r_s describes the water vapour flow resistance through the stomata of a transpiring crop and evaporating soil surface). The reference evaporation method referred to as the FAO Penman-Monteith method was published by the Food and Agriculture Organization (FAO) in Irrigation and Drainage Paper No. 56 and has been used widely for estimating grass reference evaporation using automatic weather station measurements (AWS). The AWS measurements used by the method are: solar irradiance (W m^{-2}), air temperature (^{o}C), relative humidity (%) and wind speed (m s^{-1}) and all sensors mounted at a height of 2 m. The FAO-56 Penman-Monteith equation (Allen *et al*., 1998) for measuring ET_{o} (mm) is expressed as:

$$ET_o = \frac{\Delta . r_a (R_n - G) + \rho_a C_p \delta e}{(\Delta r_a + \gamma (r_s + r_a))(\rho_w L_v)} \tag{2.15}$$

where Δ is the slope of the saturation water vapour pressure at the surface temperature (kPa ^{o}C^{-1}), R_n the net irradiance (W m^{-2}), G the soil heat flux (W m^{-2}), ρ_a the density of air (kg m^{-3}), C_p the specific heat capacity of air (J kg^{-1} K^{-1}), γ the psychrometric constant (kPa ^{o}C^{-1}), δe the water vapour pressure deficit (kPa), r_s and r_a the bulk canopy surface and aerodynamic resistances (s m^{-1}), respectively, ρ_w the density of liquid water (kg m^{-3}) and L_v the latent energy of vapourization.

The FAO-56 Penman-Monteith equation for ET_{o} has allowed crop coefficients K_c to be calculated by relating the measured total evaporation (ET) to the calculated ET_{o}:

$$K_c = \frac{ET}{ET_o} \tag{2.16}$$

The FAO-56 Penman-Monteith equation can be used to obtain hourly and daily time steps of ET_{o} and these hourly and daily measurements can be easily defined for various time steps during datalogger programming where various output-tables can be defined to suit the user.

However, the main uncertainty of the evaporation reference method is that the net irradiance R_n and soil heat flux G are estimated indirectly from the measured solar irradiance I_s.

2.6.4 Lysimetry

A lysimeter is a device made up of a large container filled with soil, water and dissolved solutes and plants (Howell *et al*., 1991). Lysimeters have been used for decades in many areas around the world to provide data to measure *ET* and to solve evaporation problems. There are different types of lysimeters and these include; hydraulic, volumetric and mass measurement by balancing. The art of lysimeter design and installation have been described in detail by Hellmann (1976); Mottram (1976); Howell *et al*. (1991) and Grebet *et al*. (1991). The device can be weighed at regular time intervals to determine *ET*. In lysimetry, the main water loss occurs due to transpiration through the stomata of the plant leaves and evaporation from the bare soil surface. Although lysimeters are regarded as the standard, they have several disadvantages. For instance, they are expensive (Mengistu and Savage, 2010a), destructive (large volumes of soil are disturbed), and non-portable (due to their large size) (Savage *et al*., 1997). Furthermore, lysimeter walls can impede energy transfer to the lysimeter and water percolation along the walls (Howell *et al*., 1991).

2.7 Micrometeorological techniques

Several methods of determining fluxes above surfaces exist, some of which are direct and others indirect. Some of these include: Bowen ratio, eddy covariance, flux variance, remote sensing, surface renewal and scintillometry. These methods have several advantages over lysimetry and other large scale hydrological modelling methods because they are continuous, portable, non-destructive and less independent on empirical factors. Nevertheless, the application of most methods is affected by fetch except for the HPV and SSS techniques which require scaling from individual stem measurements to a large area.

2.7.1 Fetch

Fetch is defined as the distance of traverse across a uniformly rough surface. To ensure collection of unbiased data, adequate fetch requirements have to be met for most of the micrometeorological techniques. The required fetch is measured by specifying an acceptable ratio of the measured flux to the local surface flux and has been found to be a strong function of atmospheric stability (Horst and Weil, 1993). Adequate fetch distance ensures that the surface energy fluxes from a surface under study are being measured and not from the adjacent areas. Fetch is most often dependent on the predominant wind direction. As a result, the predominant wind direction dictates the position and placement of sensors in a field so as to maximize fetch requirements (Savage *et al*., 1997).

2.7.2 Eddy covariance

Eddy covariance (EC) provides a direct measure of vertical wind speed and a scalar of interest. For example, this method requires simultaneous measurement of rapid fluctuations of vertical wind speed (w') and air temperature (T') for the computation of sensible heat (H). Meyers (2005) has defined the vertical turbulent flux as the covariance of a time series of the wind speed and concentration of a scalar entity over some time interval (30 to 60 minutes).

The averaging time interval should be long enough to capture all of the eddy motions that collectively contribute to the flux. The vertical turbulent flux is usually described by:

$$H = \overline{w's'} \tag{2.17}$$

where w' is the vertical wind speed fluctuation and s' is the fluctuation of the concentration of the scalar of interest and the over bar represents a time average computation.

EC method is an application of statistics and as a result it has uncertainties associated with the sampling of the atmospheric variables in order to get an estimate of the flux. Some of the biases result from sensors in which there are systematic drifts in calibration constants. Other sources of errors may result from dirt accumulation on the delicate and expensive instrument parts. Corrections are sometimes necessary to account for sensor separation and sensor path averaging (Meyers, 2005). The EC method also requires cautious sensor positioning and alignment (Mengistu and Savage, 2010a).

2.7.3 Bowen ratio energy balance method

Bowen ratio is the ratio of sensible heat H to latent heat flux LE both measured in (W m^{-2}). It is determined by the psychrometric constant multiplied by the ratio of the time-averaged profile air temperature and water vapour pressure differences. The vertical flux of water vapour, LE (W m^{-2}) is usually calculated from 20 or 30-min averages of measurements of the Bowen ratio, and other components of the energy balance. This energy balance technique is based on the assumption of similarity principle between the exchange coefficients for latent and sensible heat and it has been found to have some limitations (Savage, 2010a).

The Bowen ratio is defined as *β:*

$$\beta = \frac{H}{LE} \tag{2.18}$$

where *H* and *LE*, (W m^{-2}) mean the usual terms of the energy balance defined previously. The sign of *β* depends on the direction of the sensible heat and latent energy fluxes. In summer *β* values normally lie between 0 and 2 for most agricultural surfaces but they have been found to exceed 2 in winter. The size of the ratio depends upon the proportion of available energy directed into evaporation and sensible heat transfer. As a result, the value of *β* changes diurnally and seasonally. It has been observed that winters comprise larger sensible heat component while summers larger latent energy component due to heat lost by the latent energy exchange through evaporation of the available water (Savage *et al*., 1997; Mengistu and Savage, 2010b).

Several limitations of the Bowen ratio energy balance (BREB) method have been presented in detail by Savage *et al*. (1997). These consist of the theoretical, practical, and the boundary layer limitations.

2.7.3.1 Theoretical limitations

Using the BREB method, the computation of *LE* tends to infinity as the Bowen ratio approaches -1 due to the formulation of the theory. This has been observed when examining the denominator (1+*β*), which may not always be zero. As *β* tends to -1, this normally occurs in the early morning and late afternoon times when the available energy tends to zero due to the low values of net irradiance R_n. Rainfall events and condensation on sensors have been noticed to have similar effects.

2.7.3.2 Practical limitations

It has been pointed out that the measured differential in water vapour pressure and air temperature across the vertical distance used must be larger than the resolution of the individual sensors for unbiased results to be obtained. Depending on the prevailing conditions, it is therefore recommended to adjust the distance between the measuring arms to maintain differences above the resolution limits. Other limitations are presented by the condensation of dew on the sensors as well as post rain-events. Data loss occurs during morning periods until all the dew is evaporated (Savage *et al*., 1997; Savage *et al*., 2009).

2.7.3.3 Boundary layer limitations

In most cases, the area under study may be too small to satisfy the fetch requirements (see Section 2.8.1). For measurements taken up to 1 m above ground, 50 to 100 m of uniform upwind fetch is required (Savage *et al*., 1997; Savage *et al*., 2009). This means that predominant wind directions have to be taken into consideration to maximise fetch distances.

2.7.4 Flux variance

The flux-variance (FV) method is an indirect method based on Monin-Obukhov Similarity Theory (MOST). The FV method is attractive because it allows the estimation of H with a minimum number of routinely measured meteorological variables (Wesson *et al*., 2001). When this method is applied to estimate sensible heat flux H, it is referred to as temperature–variance (TV) method. This is because the method uses the standard deviation of high frequency air temperature measurements only and does not need wind speed measurements (Abraha, 2010).

2.7.5 Scintillometry

Surface energy balance and water budgets are important in many micrometeorological processes and have been estimated with reasonable accuracy over homogeneous surfaces using various techniques. However, fluxes determined for large areas are difficult to achieve as terrains are often heterogeneous. Unlike other point measurement methods, scintillometry has allowed measurement of path-averaged fluxes to be performed at scales of several hundred (Surface Layer Scintillometry, SLS) or thousands (Large Aperture Scintillometry, LAS) metres (Odhiambo and Savage, 2009; Savage, 2009). However, the cost of the instrumentation (scintillometer) is very high. This method involves the use of a scintillometer which is defined as an optical instrument that is made up of a radiation source (transmitter) and a receiver which consists of a sensitive detector. The transmitter and the receiver are both connected to a signal processing unit (SPU) or datalogger that records the intensity of fluctuations of the radiation after propagation through a turbulent medium (Odhiambo, 2007).

When a scintillometer is operated, the transmitter unit creates a beam of radiation which is transmitted over a defined path and the fluctuations in the radiation intensity at the receiver unit are analysed, having been influenced by variations in refractive index along the path (Hill, 1992).

2.7.6 Surface renewal

Surface renewal (SR) for estimating sensible heat *H* is a novel method for determining fluxes because it is inexpensive and simple. This method is based on observations of canopy turbulence and time-space scalar field associated with recognisable, repeated and spatially large turbulent coherent structures (Paw U *et al*., 2005). SR is based on the theory that an air parcel near a surface under investigation is renewed or displaced by an air parcel from above. The estimation of sensible heat fluxes using SR involves high frequency air temperature measurements using unshielded and naturally-ventilated fine-wire thermocouples. According to Paw U *et al*. (2005), the high frequency air temperature fluctuations results in coherent structures which resemble ramp events (Fig. 2.1). It has been reported that these coherent structures are responsible for transportation of momentum, heat and other scalar quantities of interest.

The sensible heat flux *H* is estimated from the high frequency air temperature fluctuations measured at a point above a surface of interest. The latent energy flux *LE* is then obtained as the residual of the shortened energy balance equation assuming closure is met.

Paw U *et al*. (2005) have defined the structure function, which has been used widely in turbulence data interpretation. High frequency air temperature measurements at frequency f allow air temperature structure functions of order n to be calculated, S^n (r):

$$S^n(r) = \frac{1}{m-j} \sum_{i=1+j}^{m} \left[\left(T_i - T_{i-j} \right)^n \right] \quad (2.19)$$

$$r = j / f \quad (2.20)$$

where m represents the number of data points, j the sample lag, T_i the air temperature at time i and $T_{i\text{-}j}$ at time i-j. The sample lag corresponds to a time lag (r) in seconds and this is determined by the frequency of air temperature measurement. For instance, if the frequency (f) of measurement is 10 Hz and j = 2, then the resultant time lag r = 0.2 s.

Repeated patterns like the ones found in ramps in the scalar traces have been found to create unique patterns in structure functions which resulted in further relationships between the higher moments (Fig. 2.1) (Paw U *et al*., 2005). To make these relationships simpler, Paw U *at al*. (2005) also assumed that ramps were regular patterns of fixed geometry that had instantaneous terminations for unstable conditions (the slow temperature rise would be terminated by instantaneous air temperature decrease), and for stable conditions, the slow air temperature decrease would be terminated by an instantaneous air temperature rise (Fig. 2.2).

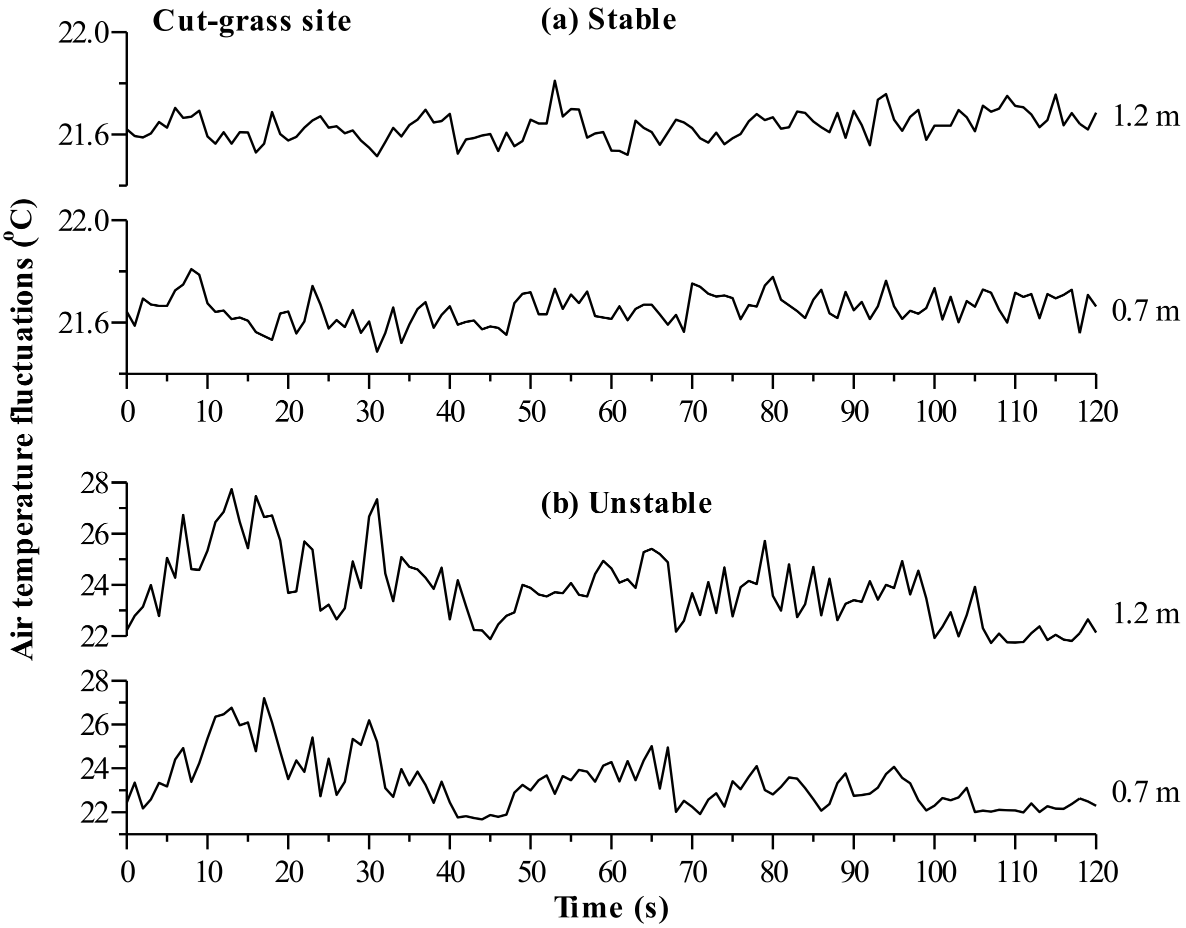

Fig. 2.1 High frequency air temperature fluctuations exhibiting ramps in a sample of 120 s of 10-Hz air temperature traces for: (a) stable (16h00) and (b) unstable (12h00) atmospheric conditions for (July 29, 2008). The high frequency air temperature measurements were at two fine-wire thermocouple heights (1.2 and 0.7 m) above ground surface at the cut-grass site.

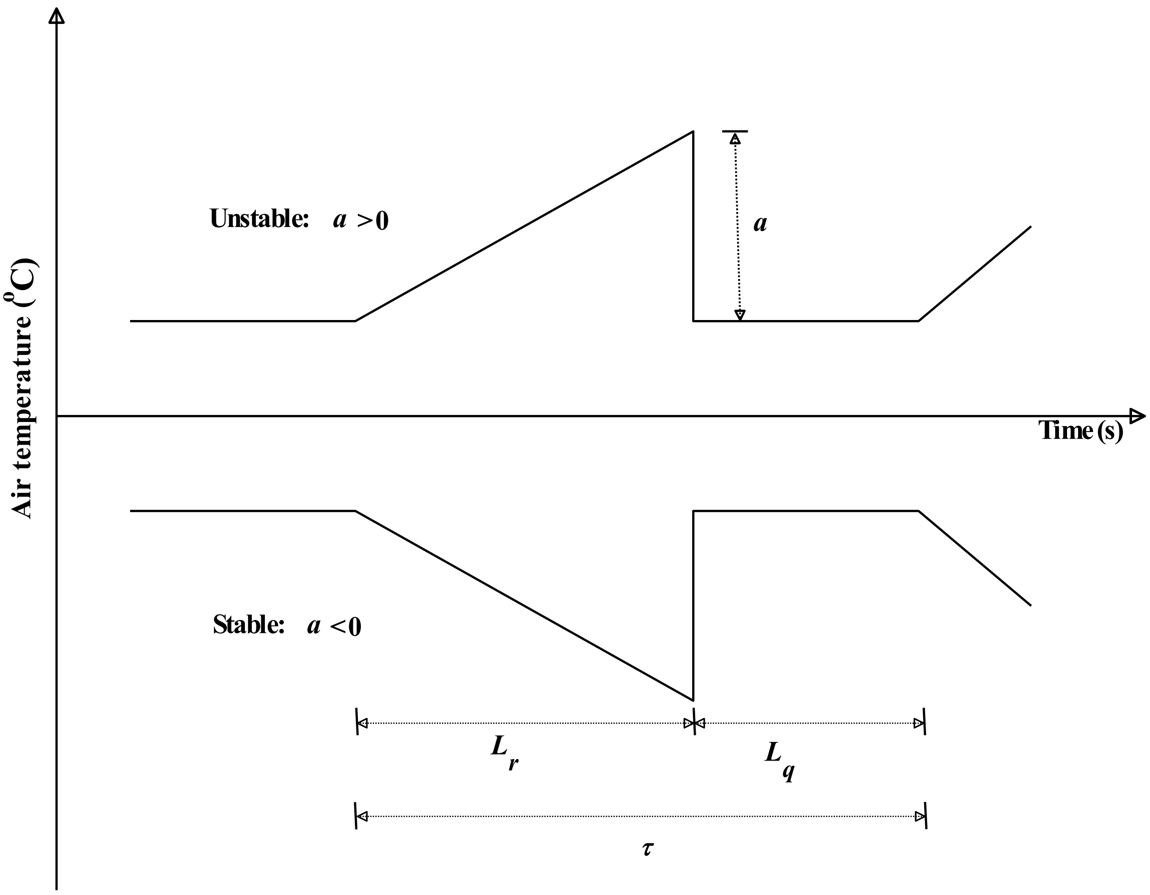

Fig. 2.2 Schematic air temperature ramps with amplitude a > 0 for unstable and a < 0 for stable atmospheric conditions. L_r is the ramp period and L_q the quiescent period while $\tau = L_r + L_q$ giving the total ramp period.

As a result, the geometry of a ramp consists of a (°C) (the amplitude of the ramp pattern), L_r (s) (a ramp period for which air temperature changes with time), L_q (s) (a quiescent period for which there is no air temperature change with time) and τ (s) (the total ramp period which the summation of L_r and L_q) (Snyder *et al.*, 1996; Mengistu and Savage, 2010a).

There are two height measurements considered in SR analysis, some height above a surface being investigated and a height representing the entire surface. For the SR method, vertical motions are not followed. As described by Paw U *et al*. (2005), the sensible heat flux H during a coherent structure is expressed as:

$$H = \alpha\rho c_p \frac{dT}{dt}\left(\frac{V}{A}\right) \tag{2.21}$$

where α is the SR weighting factor, ρ the air density (kg m^{-3}), c_p the specific heat capacity of air at constant pressure (J kg^{-1} K^{-1}). The time derivative (dT/dt) is the rate of change in air temperature (^{o}C s^{-1}). It represents the heating during the time period of a ramp only and during the spacing between ramps, no heating occurs. The ratio V/A is the volume of air per unit horizontal area. For a parcel in a canopy V/A would correspond to the measurement height z. For air temperature recorded at the canopy top, sensible heat flux by surface renewal may be determined as:

$$H = \alpha\rho c_p \frac{dT}{dt} z \tag{2.22}$$

In Eq. (2.21), T is the temperature measured at the measurement height, z the measurement height at the top of the canopy and α the SR weighting factor embodying air temperature variation in the canopy (α is a correction factor for unequal heating of cooling below the air temperature sensor). The weighting factor depends on the measurement height (z), canopy structure and atmospheric conditions (Mengistu and Savage, 2010a). Occurrences of advection or any other processes not described in SR analysis are also included in the weighting factor α which needs to be determined.

The SR method is relatively inexpensive as it does not require use of expensive and delicate instruments like other micrometeorological methods. It is a simple method that requires a point measurement of air temperature together with other energy balance components for the computation of sensible heat and latent energy fluxes. However, the method requires that the SR weighting factor α be determined by other standard measurements such as eddy covariance (Snyder *et al.*, 1996).

In this study, using fire and mowing as treatments applied to a mixed grassland site, EC and SR methods were used to investigate the altered surface radiation and energy balances. The EC method is used for determining sensible heat flux H_{EC} (Chapters 3, 4 and 5). A four-component net radiometer is used to investigate the influence of fire on the surface radiation balance (Chapter 5). An ideal SR analysis method is used for determining H_{SR} and compared to H_{EC} (Chapter 6).

Chapter 3: Energy balance of a tall grassland using eddy-covariance

3.1 Introduction

An understanding of the partitioning of the surface radiation and energy balance components and subsequent quantification of total evaporation *ET* at the Earth's surface is important in agriculture, micrometeorology and water resource management (Sumner and Jacobs, 2005; Gasca-Tucker *et al*., 2007; Villa Nova *et al*., 2007). A better understanding of the energy balance dynamics is also important for upgrading regional and global climate models (Twine *et al*., 2000). Furthermore, numerical weather models require more precise information on various surface radiation and energy balance characteristics (Hurtalová and Matejka, 1999). Thus, results of local microclimate studies on naturally occurring grasslands can be useful in model evaluation and validation.

Grasslands are one of the most abundant vegetation types in the world making up about 40% of the universal land surface (Novick *et al*., 2004; Emmerich, 2007). *ET* from natural grasslands has been shown, on average, to be approximately 300 mm per annum (Baldocchi *et al*., 2004) and locally, an average of 530 mm per annum has been recorded for a semi-arid area (Snyman, 1999). This makes them very important part of ecosystems for the exchange of energy fluxes between land surface and atmosphere (Hunt *et al*., 2002). Furthermore, grasslands provide nutritious pastureland for animals (Gasca-Tucker *et al*., 2007).

Sensible heat *H* and latent energy *LE* fluxes may be determined using various micrometeorological methods such as: eddy covariance (EC), surface renewal (SR), flux variance (FV), optical scintillation and Bowen ratio energy balance (BREB). EC is regarded as a direct method (standard for flux measurements) and uses high frequency measurements, typically three dimensional wind speeds and scalar of interest (e.g. air temperature, water vapour pressure and CO_2). This method has several limitations: it is complex, expensive and uses delicate equipment prone to damage. Some investigations have shown that eddy covariance fluxes are underestimated over some surfaces resulting in lack of closure of the surface energy balance (Twine *et al*., 2000). The SR method is a relatively simple and inexpensive method used to estimate *H* over surfaces. The SR method uses high frequency air temperature measurements, typically 2 to 10 Hz. The surface renewal method has been used successfully over different natural surfaces in South Africa (Savage *et al*., 2004; Mengistu, 2008; Mengistu and Savage, 2010b). Other micrometeorological methods are discussed in detail in Chapter 2. By contrast, a surface layer scintillometer (SLS) provides path-averaged measurements of sensible heat over distances between 50 and 300 m. The disadvantage of this method is that it is very expensive. A detailed review of theory of SLS applications has been described elsewhere (Odhiambo, 2007; Savage *et al*., 2010).

The objective of this chapter is to quantify the energy balance components for a natural tall grassland surface using the EC method with evaporation estimated as a residual of the shortened energy balance equation.

3.2 Materials and methods

The fieldwork for the experiment was conducted at the Ukulinga (29.67 ^{o}S, 30.40 ^{o}E) with an elevation of 840 m above sea level, University of KwaZulu-Natal research farm, Pietermaritzburg, South Africa. The research site is located 12 km south of Pietermaritzburg.

3.2.1 Vegetation

The vegetation of the area into which the experimental site falls has been described as Southern Tall Grassveld (Dillon, 1980; Fynn *et al*., 2004). The area has two dominant grass species, *Themeda triandra* and *Hyparrhenia hirta. Themeda triandra* flowers in early summer followed by *Hyparrhenia hirta* later in the season. Other grass species that occur in the area are *Heteropogon contortus*, *Eragrostis racemosa* and *Aristida junciformis. Aristida junciformis* is known to invade this vegetation type under most forms of disturbance. The area was 4.5 ha by size and had a fetch of 77 m from the dominant wind direction. The larger portion of the grassland area is cut for hay whilst the remainder is reserved for long-term fertilizer, burn and mowing experiments.

3.2.2 Climate

The climate of Pietermaritzburg is sub-tropical and humid with summer rainfall with a mean annual rainfall of 694 mm (Fynn *et al*., 2004). Rain occurs mainly between September and April and varies in intensity from light drizzle to heavy thunderstorms. The summers at Ukulinga are warm to hot and the winters are mild. Wind in this area is very variable and often changes direction during the day but the predominant wind direction was found to be South East.

3.2.3 Topography and soil characteristics of study site

The experimental site is relatively flat. The soils are loamy in nature and are underlain largely by Ecca shale and the occurrence of dolerite intrusions is common in this area (Dillon, 1980). The soil form that occurs at the site is mainly Bonheim. The soil is dark in colour and gaps on the ground are a common feature. Cracks are caused by shrinking and swelling of the soil during the drying and wetting cycles.

3.2.4 Measurements

The experiment was carried out from March to December 2008 over a homogeneous grassland site. The data were collected from two different plots. The vegetation in one plot was not disturbed (tall-grass site) while the remaining plot was mowed (cut-grass site). The tall-grass site was later burnt in winter and the data collection resumed the following day after the burning. Each site was equipped with a three-dimensional sonic anemometer (RMY81000, R.M. Young, Traverse City, MI), placed at a 2 m height above the ground surface (Fig. 3.1). This instrument has a path length of 100 mm. The sonic anemometer was installed vertically supported by a boom attached to a mast and a spirit-level was used to check the vertical alignment of the sensor relative to ground surface. The sonic anemometer was connected to a CR3000 datalogger (Campbell Scientific, Logan, Utah, USA) for the tall-grass site and CR5000 for the cut-grass site. High frequency data, two-

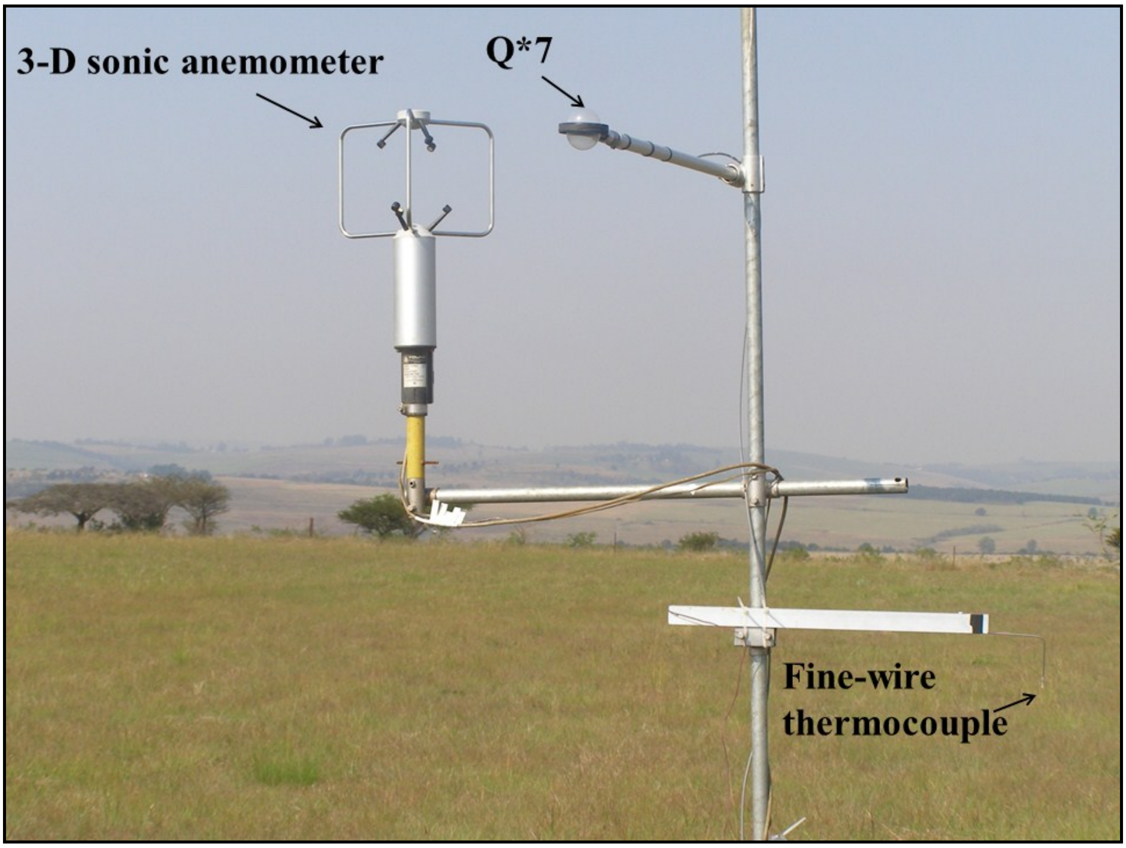

Fig. 3.1 R.M. Young (model 81000) 3-D sonic anemometer, net radiometer (Q*7) and surface renewal (SR) unshielded fine-wire thermocouple supported above a short grass canopy by a horizontal boom joined to a mast.

min and 30-min averages of three-dimensional wind speed velocity components *u, v, w,* sonic temperature T_s, wind direction and the covariances between w and T_s were processed online in the datalogger and stored for further data analysis.

Post-data corrections included coordinate rotation of axes, water vapour pressure (e) effects on sonic temperature and β (ratio of H to LE) corrections. Using coordinate rotation is important before H_{EC} measurements can be used to represent various surface fluxes. This is because before rotation the measured fluxes are susceptible to instrument errors due to tilt relative to the nature of the landscape or tower structure. The effects of coordinate rotation, e and β corrections are presented in Chapter 4. Other components of the energy balance were also measured at the tall-grass site. The net irradiance R_n was measured using a Q*7 net radiometer (REBS, Seattle, Washington, USA) placed at 2 m above ground. Initially, ECH_2O probe sensors (Decagon Devices, Pullman, Washington, USA) were used to measure soil water content at a depth of 0.06 m below the soil surface. Subsequently, two additional sensors, ThetaProbe (model ML2, Delta-T Devices, Cambridge, UK), were used to also measure soil water content at each site (Fig. 3.2). Two soil heat flux plates (model HFT-S, REBS), buried at 0.08 m depth below the soil surface, placed about 1 m apart were used to measure soil heat flux.

Fig. 3.2 ThetaProbe (A) and ECH_2O Dielectric Aquameter (B) used for measuring soil water content.

A set of parallel-thermocouples at depths of 0.02 and 0.06 m were used to measure average soil temperature and later used to compute the temporal change in soil temperature. This was used to calculate the soil heat flux stored above the soil heat flux plates. All these sensors were connected to the CR3000 datalogger and the data averages stored every 2 and 30 min.

The surface renewal (SR) method was used at both the tall- and the cut-grass sites. The SR method consisted of two unshielded and naturally ventilated 75-μm diameter type-E fine-wire thermocouples for air temperature measurement. The thermocouples were supported by an aluminium boom attached to the main mast supporting the sonic anemometer (Fig. 3.1). The placement heights for the fine-wire thermocouples were 0.7 and 1.2 m above the soil surface (the grass was 0.2 m tall for the cut-grass site). The air temperature measurements for the SR analysis were sampled at the same frequency as the sonic anemometer. The air temperature measurements were lagged by 0.4 and 0.8 s before the second, third and fifth air temperature structure functions were computed online. The time lags (0.4 and 0.8 s) have been found to yield successful results by other studies (Mengistu, 2008; Mengistu and Savage, 2010a; 2010b; Nile, 2010. The fine-wire thermocouples were connected differentially to the CR3000 datalogger used by the sonic and the same data output used. Data collected using SR method will be discussed in detail in Chapter 6.

3.2.5 On-site automatic weather station

An automatic weather station (AWS) was installed at the tall-grass site and the factors that quantify the microclimate: (solar irradiance (I_s), air temperature (^{o}C) and relative humidity (%) and wind speed (U) were obtained. Additional measurement of rainfall was also obtained from the AWS. Water vapour pressure *e* (kPa) was calculated from air temperature and relative humidity measurements online. All AWS sensors were connected to a Campbell CR10X datalogger. The logger programme was set at a scan rate of 10 s and output averages every 10 min, hourly and daily were obtained.

3.3 Results and discussion

3.3.1 Weather variables at the experimental site

Some of the data collected from the automatic weather station (AWS) at the experimental site, graphically displayed in Fig. 3.3, illustrate the variable microclimate during 2008. The grass reference evaporation (ET_o) mm computed from the AWS data exceeded the rainfall most of the time (Fig 3.3 (c)). The ET_o for the duration of the experiment (March to December 2008) was 781.7 mm. Conversely, the total amount of rainfall received was only 450.3 mm. The contribution of the grasslands to the hydrological cycle is undisputable as ET_o exceeds rainfall at the experimental site. The effect of solar irradiance I_s on the pattern of ET_o at the experimental site is shown on Fig. 3.3 (b). The daily curve of ET_o and total I_s (MJ m^{-2}) followed the same pattern. This shows how important solar irradiance is in regulating the exchange of energy between the Earth's surface and the atmosphere. Minimum and maximum air temperature (*Tmin* and *Tmax*) also varied diurnally depending on the prevailing weather conditions (Fig 3.3 (a)).

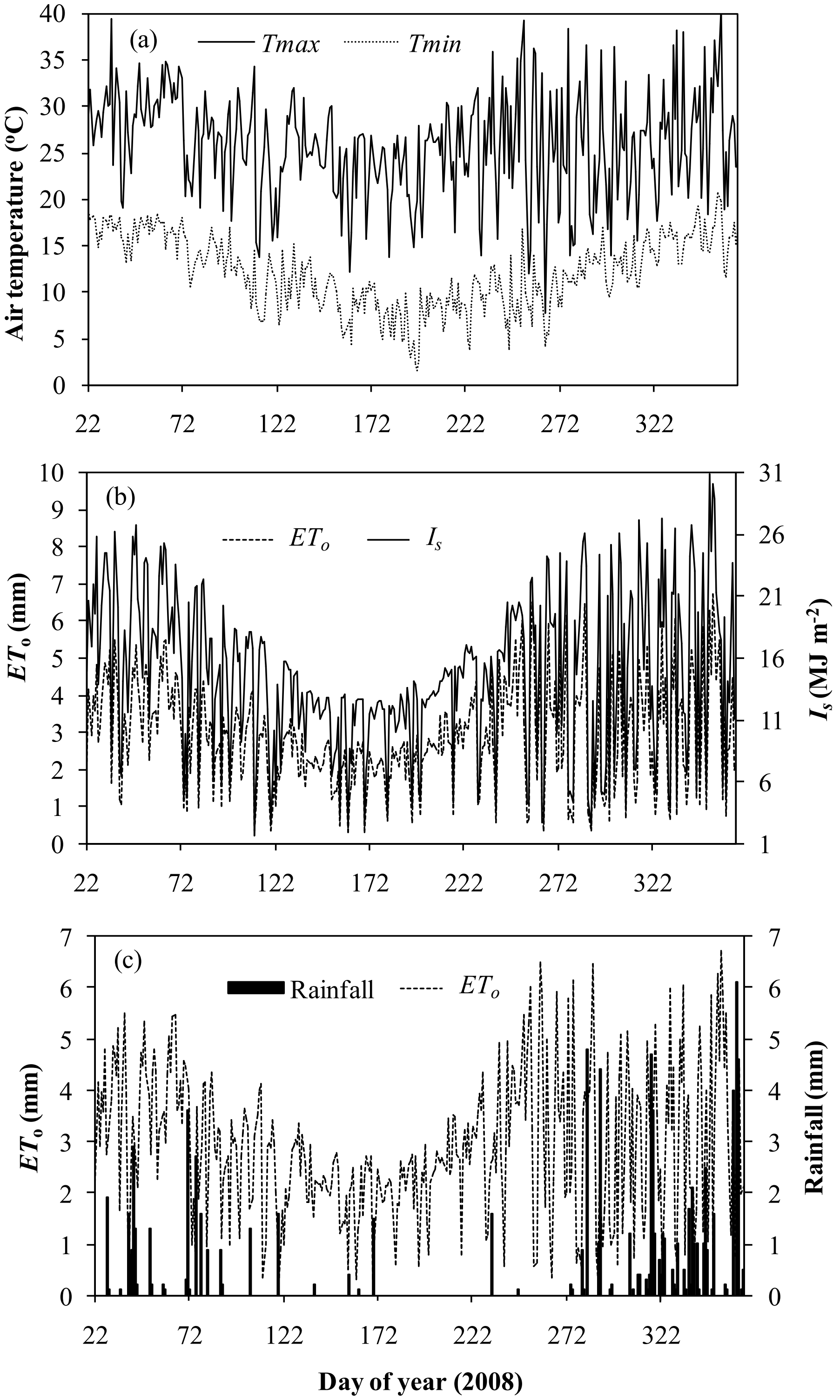

Fig. 3.3 Temporal variation of (a) daily maximum *Tmax* and minimum *Tmin* air temperature (°C), (b) daily grass reference evaporation and total solar irradiance (MJ m^{-2}) and (c) daily grass reference evaporation (mm) and total rainfall (mm) during the experimental period (2008) at Ukulinga, Pietermaritzburg, South Africa.

3.3.2 Surface energy balance measurements

Three energy balance measurements R_n, H_{EC} and G were collected over a period of four months (March, April, May and June), Table 3.1. The latent energy flux (*LE*) was estimated as a residual of the shortened energy balance equation (Eq. (2.9)).

There was a noticeable trend of decreasing energy balance components with the approach of winter. The net irradiance (R_n) measured at the tall-grass site was the highest followed by the sensible heat (*H*) and *LE*. The soil heat flux (*G*) was the lowest measured energy balance component for the months (March to May) whilst in June the *G* term became higher than the *LE* component as the available R_n became less or probably due to absence of rainfall and soil water. The diurnal variation of the four fluxes over selected days in winter is shown in Figure 3.4 for the tall-grass site. Day of year 164 to 167 had cloudless skies while DOY 168 and 169 where cloudy. Daily total variations of the fluxes are also presented in Figure 3.5.

Daily averages of Bowen ratio and total evaporation (*ET*) were calculated for naturally growing grassland using eddy covariance method and these changed diurnally with prevailing atmospheric conditions (Fig. 3.6). Typically, cloudless days were characterised by high values of *ET* while the corresponding Bowen ratio was low. High *LE* meant that the Bowen ratio will be small as *LE* is the denominator. *ET* was relatively high in March and April but it steadily decreased in May and June as the available energy became reduced as the season changed to winter.

Table 3.1 Daily values for March (DOY 80 to 86), April (DOY 101 to 119), May (DOY 130 to 134) and June (DOY 155 to 172) of net irradiance (R_n), eddy covariance sensible heat flux (H_{EC}), soil heat flux (G), latent energy flux (LE), total evaporation (ET), reference evaporation (ET_o), available energy (R_n–G) and Bowen ratio (β). Flux values of R_n, H_{EC}, LE and G are daily summations for unstable conditions only when all terms are positive.

DOY (2008)		Energy balance components							
		R_n (MJ m^{-2})	H_{EC} (MJ m^{-2})	G (MJ m^{-2})	LE^a (MJ m^{-2})	ET^b (mm)	ET_o (mm)	R_n - G (MJ m^{-2})	β^c
	Tall grass site								
80		3.80	1.44	0.58	1.78	0.73	4.14	3.22	0.81
81		7.56	2.37	2.03	3.16	1.30	0.94	5.53	0.75
82		13.36	5.12	2.72	5.52	2.27	2.34	10.64	0.93
83	March	13.90	5.33	3.04	5.53	2.27	3.94	10.86	0.97
84		10.05	4.83	1.86	3.36	1.38	4.35	8.19	1.44
85		8.45	3.84	1.85	2.76	1.13	2.84	6.60	1.39
86		9.42	4.44	2.30	2.68	1.10	2.63	7.12	1.66
	Total	**66.54**	**27.37**	**14.38**	**24.79**	**10.20**	**21.18**	**52.16**	
101		6.94	2.99	1.43	2.51	1.03	3.64	5.51	1.19
102		10.13	5.46	1.54	3.12	1.28	3.44	8.58	1.75
103		5.72	3.30	0.92	1.50	0.62	3.27	4.80	2.19
106		10.59	5.00	1.61	3.98	1.64	1.69	8.98	1.26
107		10.08	4.67	1.52	3.89	1.60	1.88	8.56	1.20
108		10.33	4.98	1.63	3.72	1.53	3.10	8.70	1.34
109	April	9.99	4.46	1.92	3.61	1.49	3.33	8.07	1.23
111		3.58	3.24	0.02	0.32	0.13	0.35	3.56	-
113		9.76	5.14	1.52	3.10	1.28	1.00	8.24	1.66
114		9.61	4.52	1.73	3.37	1.39	2.90	7.88	1.34
115		9.45	4.08	1.83	3.54	1.46	2.97	7.62	1.15
116		8.28	3.82	1.69	2.77	1.14	2.87	6.60	1.38
117		7.59	4.27	1.45	1.86	0.77	3.42	6.14	2.29
118		1.59	0.40	0.11	1.08	0.44	2.96	1.49	0.37
119		3.58	1.27	0.52	1.78	0.73	1.99	3.06	0.71
	Total	**117.22**	**57.61**	**19.44**	**40.17**	**16.53**	**38.81**	**97.79**	
130		5.64	2.21	1.35	2.09	0.86	3.36	4.30	1.06
131		7.93	3.69	1.14	3.11	1.28	2.33	6.80	1.18
132	May	7.87	3.82	1.12	2.94	1.21	3.13	6.76	1.30
133		6.90	4.02	0.92	1.95	0.80	2.59	5.98	2.06
134		6.34	2.93	0.95	2.47	1.02	1.80	5.40	1.19
	Total	**34.69**	**16.67**	**5.46**	**12.56**	**5.17**	**13.21**	**29.23**	
155		1.94	1.18	0.16	0.60	0.25	1.93	1.78	1.95
156		7.33	3.73	0.51	3.09	1.27	0.49	6.82	1.20
157		7.11	3.72	0.62	2.76	1.14	2.03	6.48	1.35
158		7.12	3.53	0.96	2.62	1.08	2.12	6.15	1.35
159		1.32	0.18	0.05	1.09	0.45	2.49	1.27	0.17
163	June	4.50	2.99	1.08	0.43	0.18	2.52	3.42	-
164		6.78	3.45	1.77	1.56	0.64	1.56	5.01	2.21
165		6.84	3.53	2.14	1.16	0.48	2.29	4.70	3.04
166		6.77	3.60	2.13	1.04	0.43	2.71	4.64	3.45
167		6.70	3.49	2.10	1.11	0.46	2.43	4.60	3.15
172		6.80	3.74	1.91	1.16	0.48	2.64	4.89	3.23
	Total	**63.20**	**33.13**	**13.44**	**16.63**	**6.84**	**23.20**	**49.76**	

Superscripts *a*, *b* and *c* denotes components derived from total energy flux densities (MJ m^{-2}).

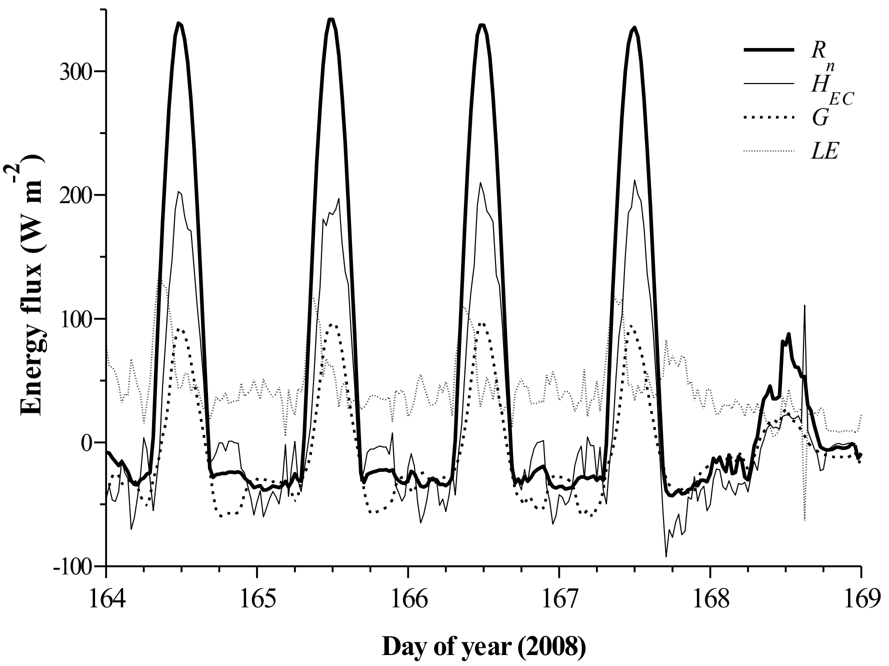

Fig. 3.4. Diurnal energy flux variations for the tall-grass site for June (2008), DOY 164 to 168. Day of year 164 to 167 had clear skies while day of year 168 had cloudy skies.

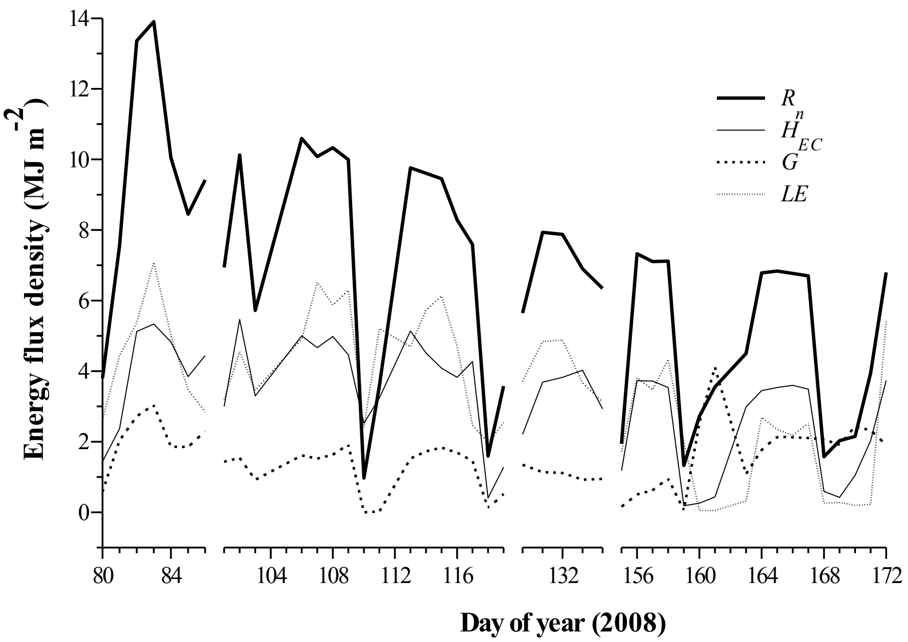

Fig. 3.5 Daily patterns of energy balance terms for a tall grass in KwaZulu-Natal midlands (South Africa).

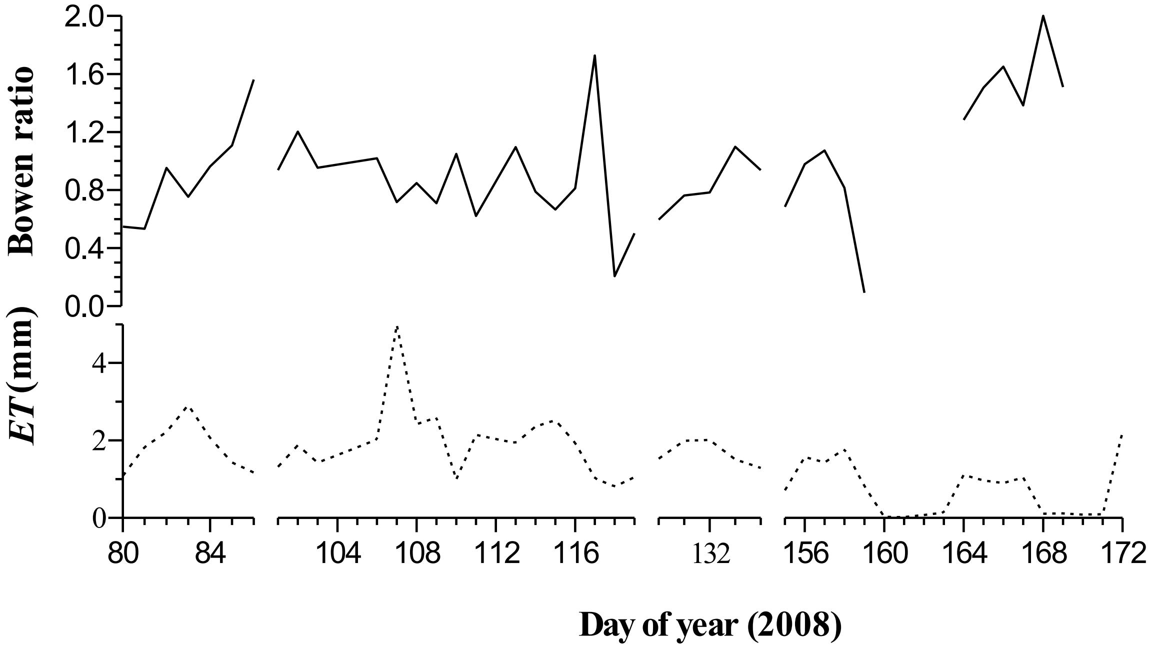

Fig. 3.6 Daily averages of the Bowen ratio and total evaporation (*ET*). The Bowen ratio and *ET* were measured at 30-min interval on selected days of March to June using EC method. Daily β values greater than 2, corresponding to cloudy and wet days, were excluded.

The grass reference evaporation (ET_o) showed a similar trend to *ET*. For example, daily values of *ET* and ET_o ranged from 0.13 to 2.27 mm and 0.35 to 4.35 mm for months (March and April), respectively, whilst winter month (June) had *ET* and ET_o range of 0.18 to 1.27 mm and 0.49 to 2.71 mm, respectively (Table 3.1). As expected, the grass reference evaporation was often greater than the *ET* estimated using EC method for all months. The grass reference evaporation exceeded *ET* because it is the amount evaporated from a hypothetical surface not short of water or nutrients (Allen *et al*., 1998) while the vegetation from which *ET* was determined may be short of water and nutrients. Similar total evaporation rates for winter months have been observed elsewhere for grassland areas during winter (Wever *et al*., 2002).

Measurements of *ET* from natural grass communities is crucial for water resource planning and limited historic data on rain-fed natural grasslands makes these estimates desirable. Several other methods (Penman-Monteith, Priestley-Taylor, grass reference evaporation and pan evaporation) of estimating *ET* have been successfully tested over grasslands (Sumner and Jacobs, 2005; Villa Nova *et al*., 2007). Most of the energy balance components changed diurnally and seasonal signal was evident as winter approached. Total *ET* measurements calculated from *LE* varied from day to day and a winter month (June) had the lowest *ET* rates. *ET* has been shown to depend on daylength and hence yielding a seasonal signal (Penman, 1948).

3.4 Conclusions

Most of the energy balance components are sensitive to changes in atmospheric conditions and the effects of clouds can easily be seen from irregular curves while a smooth diurnal curve indicates clear sky conditions. Energy balance component fluxes during night time, dawn and dusk were mostly small in magnitude due to decreased or no solar irradiance as the sun dips below the horizon. Positive fluxes only occurred during the day after sunrise and are highest at noon.

The months (March and April) had a higher peak of *ET* (2.27 and 1.64 mm per day) and ET_o (4.35 and 3.64 mm), respectively, than values observed for winter months (May and June) *ET* (1.28 and 2.71 mm per day) and ET_o (3.36 and 2.71 mm), respectively. A consistent pattern of $R_n > H_{EC} > LE > G$ was observed for most days from March to June but a relative decrease of all terms was evident as winter approached. The Bowen ratio was generally lower for months before the onset of winter. The Bowen ratio for the winter month (June) ranged from 0.17 to 3.45 whilst March and April had a range of 0.71 to 2.29 excluding wet days with almost complete cloud-cover. Greater values of Bowen ratio were expected for winter as the weather conditions became more drier compared to months before winter when total evaporation rates were generally high making *LE* higher than *H*.

In this study, the EC method gave consistent estimates of sensible heat fluxes over naturally occurring grassland. The method proved reliable for giving long-term measurements of sensible heat flux and estimates of total evaporation (calculated as a residual from the shortened energy balance equation).

Chapter 4: Influence of mowing on energy balance of a tall grassland

4.1 Introduction

In grassland communities, the choice of a particular management strategy can result in various changes to land surface properties (Wilson *et al*., 1984). Management strategies such as fire, mowing, fertilization (Dillon, 1980; Wright and Bailey, 1982; Harrington *et al*., 1984; Pearson and Ison, 1997 and irrigation (Edwards and Tainton, 1990) can have significant impacts on the composition and succession of the native grasses and may directly or indirectly affect the energy balance of a grassland community (Bremer and Ham, 1999) and therefore global climate change. Moreover, grassland management practices such as fire may affect the sequestration or release of carbon from grasslands (Bremer and Ham, 2010). The effects of fire, wind erosion and vegetation diversity on grasslands have been subject of a number of studies (Savage and Vermeulen, 1983; Bremer and Ham, 1999; Fynn *et al*., 2004; Vermeire *et al*., 2006; Wang and Davidson, 2007; Bremer and Ham, 2010). However, published information on the effects of mowing on the surface radiation and energy balance of grasslands is lacking.

Sanderson (2008) studied the effects of grazing and mowing on switchgrass yield, nutritive value, and soil carbon changes. Annual variation in weather and harvest management had significant effects on yield and nutritive value of switchgrass than did the differences in the genetic make-up of the cultivars. Soil carbon levels did not change after five years of grazing on the site with a long history of hay and pasture. However, at a site with a history of row crops, the soil carbon was found to be 33% greater after seven years under mowing management.

Adema *et al*. (2004) also studied the effects of mechanical control of shrubs in a semiarid region of Argentina and its effect on soil water content and grassland productivity. The mechanical shrub control significantly increased soil water content in the upper 1.0 m of the soil. Grass production, accumulation of surface litter and water use efficiency were also improved considerably. However, in some grass species, mowing of the grass was found to reduce above-ground plant regrowth (Limb *et al*., 2011).

The height at which the grass is mowed has been shown to have considerable effects on forage production, persistence and available soil water. Van Riper and Owen (1963) found that bromegrass yielded significantly more dry matter per unit area than orchardgrass when mowed at a 50 mm height than when mowed at 125 mm height. They also found that grasses mowed at 125 mm height had more plants per unit area than grasses cut to 50 mm. Furthermore, grasses cut to 50 mm used less water per unit of soil depth than grasses cut to 125 mm.

Native grasslands are commonly mowed for hay harvesting purposes and in most cases the grass is allowed to re-grow until the next harvest without determining the impact of such a management strategy on the microclimate and other environmental factors. Therefore the objective of this study was to determine the influence of mowing on the energy balance components of a tall grassland.

4.2 Materials and methods

4.2.1 Study area

The mowing experiment was conducted at Ukulinga (30^{o} 40'E, 29^{o} 67'S and altitude of 840 m), the research and training farm of the University of KwaZulu-Natal, Pietermaritzburg, South Africa. Rainfall in this area is more intense in spring and summer and the maximum total evaporation rates also take place during this period. A detailed account of the soil type, climate and vegetation of the experimental area is given in Chapter 3.

4.2.2 Experimental design and instrumentation

The experiment was carried out from March to December 2008. A grassland area, greater than 4.5 ha was divided into two, the cut and tall-grass sites. The cut-grass site was mowed (harvested for hay) at the beginning of the experiment while the tall-grass site remained intact until the burn towards the end of the winter season. A three-dimensional sonic anemometer (RMY81000, R.M. Young, Traverse City, MI), was set up at a height of 2 m above the soil surface at the cut-grass site. The surface renewal SR system comprising of two type-E fine-wire thermocouples (75-µm diameter) was also set up at this site. The two fine-wire thermocouples were placed at 0.6 and 1.1 m heights above the soil surface, respectively. The thermocouple measurements were made differentially and air temperature measurements sampled at a frequency of 10 Hz. The second, third and fifth air temperature structure values were obtained using time lags 0.4 and 0.8 s. The time lags (0.4 and 0.8 s) have been found to yield successful results by other studies (Mengistu, 2008; Mengistu and Savage, 2010a, b; Nile, 2010. Both the sonic anemometer and fine-wire thermocouples were connected to a CR5000 datalogger (Campbell Scientific, Logan, Utah, USA). High frequency data, 2 min and 30-min averages of three-dimensional wind speed components; u, v, w, sonic temperature T_s, wind direction and the covariances between w and T_s and air temperature structure functions data were processed online in the datalogger and stored in 1 or 2 gigabyte cards for further analysis. A surface renewal iteration spreadsheet (Savage, 2010b) was used to calculate sensible heat fluxes H_{SR} from collected air temperature structure function data.

Post-data corrections included coordinate rotation of axes, vapour pressure e (kPa) and β corrections for sonic temperature. The eddy covariance sensible heat flux H_{EC} was corrected for e and β using the following equation (Savage *et al*., 1997):

$$H_{EC} = H_s \cdot \left(1 + \frac{0.322\bar{e}}{\bar{P}} + \frac{10^{-3} \cdot (0.722\bar{P} - 0.399\bar{e})}{\beta} \right)^{-1} \tag{4.1}$$

where H_s is the uncorrected sonic sensible heat flux, $\bar{e}$ (kPa) the average water vapour pressure, $\bar{P}$ (kPa) the average atmospheric pressure and β the ratio of H_s to LE. The atmospheric pressure P was calculated from:

$$P = \frac{-e(M_d - M_w) + M_d P_o}{RT + M_d gh} \tag{4.2}$$

where e (kPa) is the water vapour pressure calculated from measurements of air temperature and relative humidity, M_d and M_w (g mol^{-1}) are the molecular masses of dry air and water, respectively, P_o (Pa) the atmospheric pressure at sea level, R (J mol^{-1} K^{-1}) the universal gas constant, T (K) the air temperature or T_a, g (m s^{-2}) the acceleration due to gavity and h (km) the height above sea level and hence:

$$P = \frac{-0.01094866e + 2934.7773}{8.31451(T_a + 273.15) + 0.28362157h} \tag{4.3}$$

A detailed formulation of total atmospheric pressure can be found in Savage *et al*. (1997).

Additional measurements required for the computation of the energy balance components were also obtained for the cut-grass site. The net irradiance R_n was measured using a Q*7 net radiometer (REBS, Seattle, Washington, USA), placed at 2 m above the soil surface and facing north. At the beginning of the experiment, ECH$_2$O probe sensors (Decagon Devices, Pullman, Washington, USA), were used to measure the soil water content for both sites. The ECH$_2$O sensor for the tall-grass site read poorly due to bad contact between the sensor and the soil resulting in a very low soil water content measurement. The CR5000 programme was later on modified to accommodate two additional ThetaProbe sensors (model ML2, Delta-T Devices, Cambridge, England, UK), used to measure soil water content. Subsequent results proved to be successful as the soil water content measurements for both sites were similar. Two soil heat flux plates (model HFT-S REBS), buried at 0.08 m below the soil surface, placed 1 m apart were used to measure the soil heat flux *G*. Two sets of type-E parallel-thermocouples were installed at 0.02 and 0.06 m depths to measure the average soil temperature above the soil heat flux plates. The average soil temperature above the plates was used to compute the soil heat flux stored above the soil heat flux plates. All the sensors were connected to one datalogger at each site. Output data intervals were every 2 and 30-min.

4.3 Results and discussion

4.3.1 Soil water content

The dominant grass species that occurs at the experimental site is *Themeda triandra*. At the beginning of the mowing experiment, the grass height of the native grass was 0.4 m. The tall grass was cut to a height of 0.1 m. The excess litter resulting from the cut-grass was removed using pick-up rotors mounted on a tractor (Fig. 4.1).

After mowing, the soil surface remained covered by the above ground litter layer. When this litter is deposited to the soil surface, it is transformed to humus, which is vital for water retention and nutrient cycling (Boeken and Orenstein, 2001). The average soil water content recorded from DOY 143 to 145 was 0.31 $m^3 m^{-3}$ for the cut-grass site compared to a very low value of 0.12 $m^3 m^{-3}$ for the tall-grass site (Fig. 4.2).

Fig. 4.1 Equipment used during the preparation of the cut-grass site.

The cut-grass site maintained relatively high soil water content due to the reduced leaf area index (LAI) whereas the tall-grass site maintained a low water content because it had a high leaf area index. It should be noted that LAI was not measured but only casual observations were made.

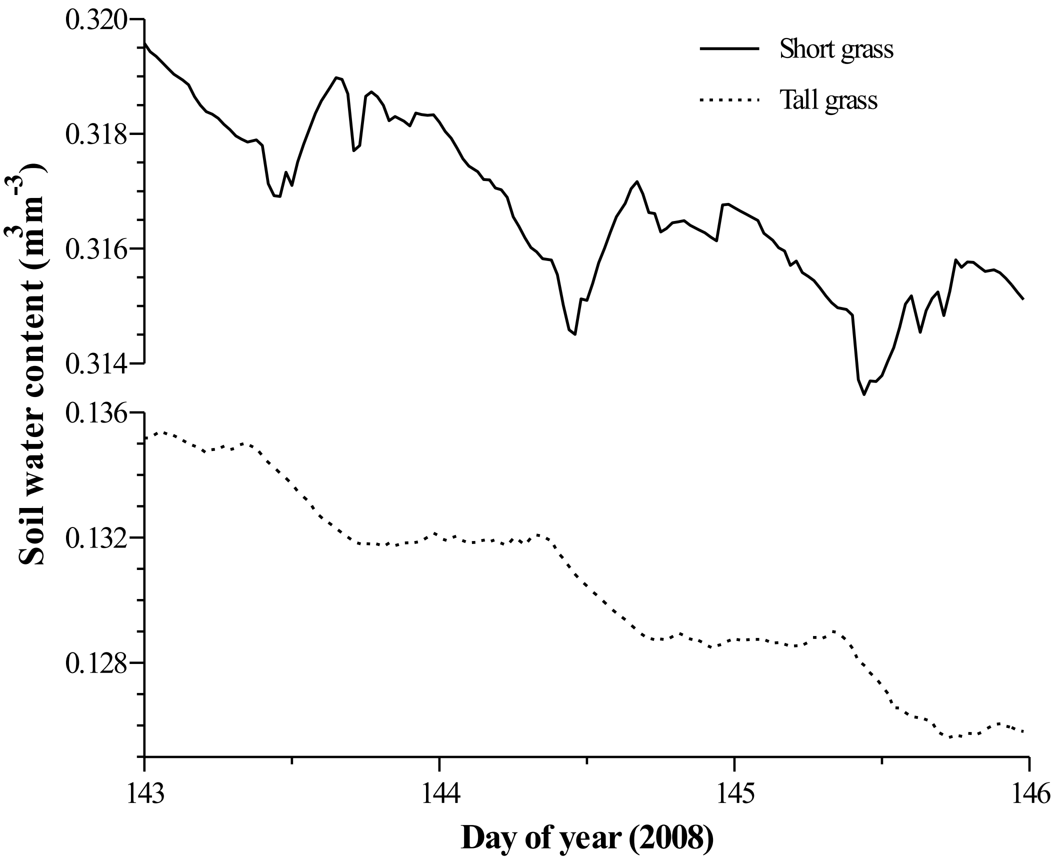

Fig. 4.2 Diurnal variations for the 30-min soil water content at the cut-grass and tall-grass sites.

4.3.2 Soil temperature dynamics

The soil temperature recorded over a three-day period (DOY 143 to 146 May 2008) at the cut-grass site was consistently high as compared to the tall-grass site for the same period (Fig. 4.3). The cut-grass site had a maximum soil temperature of 21.1 ^{o}C, minimum of 13.9 ^{o}C and an average of 16.8 ^{o}C. On the other hand the tall-grass site recorded a maximum soil temperature of 18.3 ^{o}C, minimum of 12.9 ^{o}C and an average of 15.2 ^{o}C for the same period. The mowing of the grass is likely to have led to the increase in soil temperature as more solar irradiance reached the soil surface unimpeded.

The tall-grass site generally had a low temperature due to excess litter on the soil surface that acted as a thermal insulator. The grass stands may also have provided shade thereby keeping the soil surface cool for most of the time. Temperature regimes at both sites followed a similar diurnal pattern. Maximum soil temperature was reached at 14:30 while minimums occurred at 05:30 for the cut-grass site. The tall-grass site soil temperature showed slight lagging probably due to the effect of mulching caused by the litter.

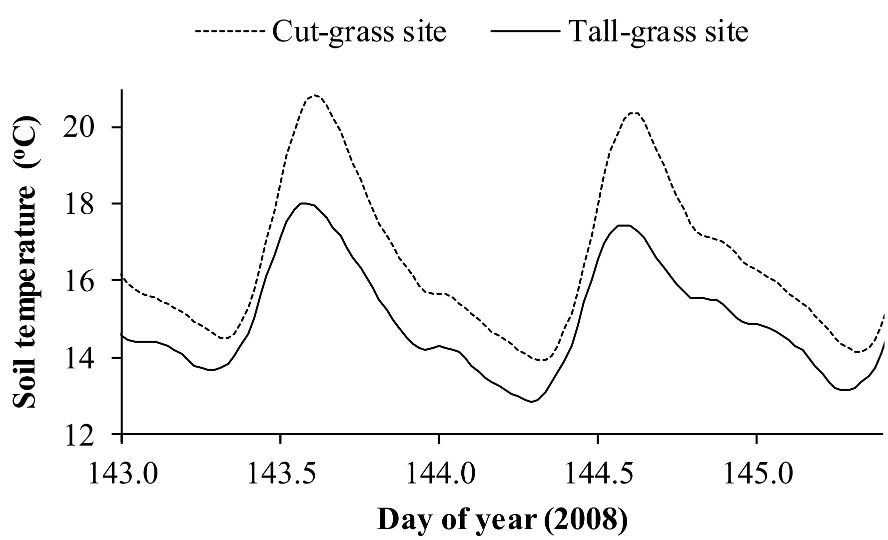

Fig. 4.3 Diurnal patterns of average soil temperature, between 0.02 and 0.06 m for the cut- and the tall-grass sites.

4.3.3 Coordinate rotation and sensible heat flux corrections

Sonic anemometers have been used over various types of terrains to measure turbulent fluxes to estimate the exchange of momentum, sensible heat and other scalar fluxes by using the EC method. The elevation at which the sonic anemometers are placed is often determined by the fetch requirements of the area as well as the vegetation heights. When employing methods such as the EC, the mast or tower geometry to use for mounting the EC systems are often decided upon by the user. Fluxes derived from EC systems are therefore susceptible to errors caused by instrument tilt relative to the underlying surface (Wilczak *et. al*., 2001; Vickers and Mahrt, 2006; Sun, 2007; Richiardone *et al*., 2008). Measurements from sonic anemometers are also affected by angle of attack errors. These errors are due to poor (co)sine response of the anemometers as a result of self-sheltering by the transducers or flow obstruction by the frame morphology of the anemometer (Nakai *et al*., 2006). The tubing that supports the transducers array has been implicated in flow distortions within the measurement volume (Mauda *et al*., 2007). The physical structure of the tower or mast used may also obstruct the flow of various measured scalars (Richiardone *et al*., 2008). The obstruction of wind velocity by the geometric structure of the tower has been referred to as tower shadowing (Olando *et al*., 2011). Instruments located in the wake of the tower are therefore likely to record measurements which under-represent the true wind conditions and subsequently distort the H fluxes, for example.

A detailed account of coordinate rotation methods and applications has been presented by Wilczak *et al*. (2001) and Finnigan (2004). The process of post-rotating sonic data is traditionally called tilt correction and allows for correction of air velocity data relative to the terrain under study (Sun, 2007). Applying coordinate rotation to the 3-D sonic anemometer is therefore crucial before the eddy covariance measurements can be adopted to represent the fluxes between the surface of interest and the atmosphere.

A two day comparison of coordinate rotated sensible heat fluxes (H_{EC_ROT}) and not rotated H_{EC} fluxes (H_{EC_NR}) is presented in Fig. 4.4. The influence of coordinate rotation is difficult to notice from the diurnal curves Fig. 4.4 (a) and (b) without doing a regression analysis between the H_{EC_NR} and H_{EC_ROT} fluxes. Fig. 4.4 (a) shows the near clear sky conditions and Fig. 4.4 (b) has more spikes indicating the influence of clouds, wind or water vapour pressure on measured scalars.

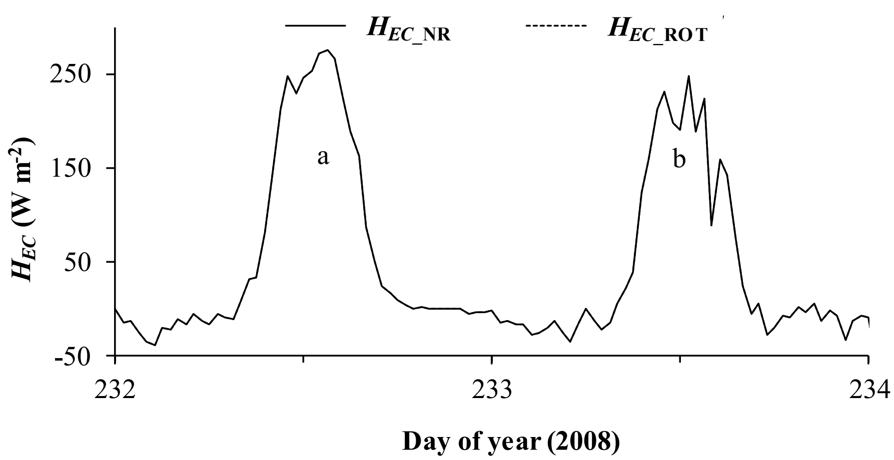

Fig. 4.4 (a) and (b) Diurnal variations for 30-min stored sensible heat flux not rotated (H_{EC_NR}) and rotated (H_{EC_ROT}) for the cut-grass site. The H_{EC_ROT} was computed from the high frequency data obtained from the 3-D sonic. A visual basic program was used to do coordinate rotation and calculate fluxes.

In addition to coordinate rotation, EC measurements also need to be corrected for water vapour pressure e (kPa) effects on the sonic temperature as well as correction for β (ratio of H to LE) (see section 4.2.2). β varies depending on the prevailing weather conditions, as a result it will vary with time of day and season. For example, if β is small then the correction is large and this often happens when LE is largest (e.g. summer). Conversely, if β is large then the correction is small (e.g. in winter). Correcting for β is therefore necessary especially when β is small. Correcting for e and β makes a substantial difference on the H_{EC} fluxes (Fig. 4.5). The $H_{EC\_\mathrm{ROT\_CORR}}$ fluxes remained lower than the H_{EC_NR} fluxes for unstable conditions and little variation was observed for stable conditions. Graph of H_{EC_NR} fluxes versus $H_{EC\_\mathrm{ROT\_CORR}}$ fluxes (Fig. 4.6 (a)) yielded an R^2 value of 0.97 while Graph of H_{EC_NR} fluxes versus H_{EC_ROT} fluxes yielded an R^2 of 0.98 (Fig. 4.6 (b)). The plotted data included both stable and unstable conditions. Most of the data lay above the 1:1 line and this indicates that the H_{EC_NR} fluxes are over estimating H. Regression analysis of H_{EC_NR} versus $H_{EC\_\mathrm{ROT\_CORR}}$ and H_{EC_ROT} fluxes was performed to illustrate the effect of coordinate rotation and water vapour pressure corrections on the EC fluxes (Table 4.1). Applying e and β corrections to the rotated H_{EC} fluxes increased the slope of the regression from 1.12 to 1.15 while the R^2 decreased by 0.01. Correcting the sensible heat fluxes for e and β decreases H_{EC} by about 15% and this may explain the pattern shown in Fig. 4.5 where the rotated and corrected fluxes were consistently lower than the not rotated and uncorrected H_{EC} fluxes.

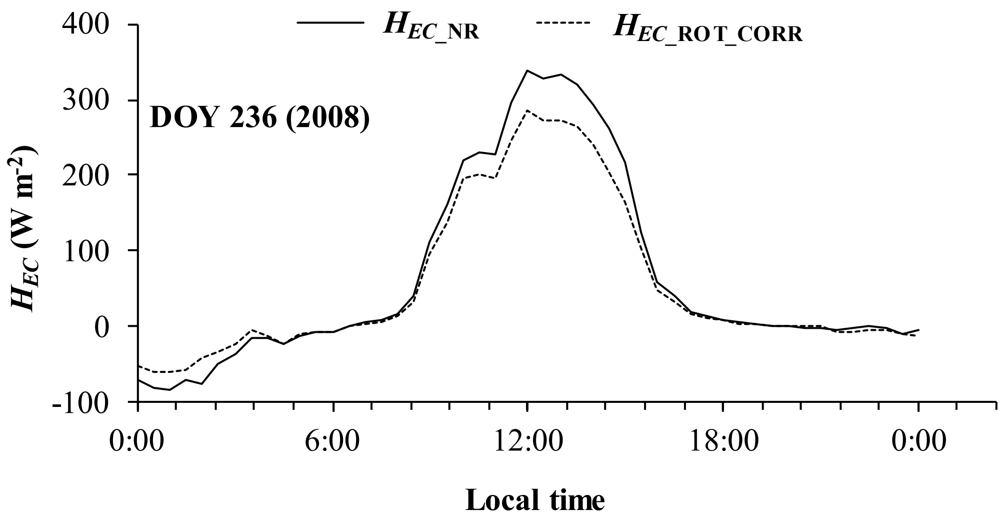

Fig. 4.5 Diurnal variation of the sonic sensible heat flux not rotated (H_{EC_NR}) and sonic heat flux rotated and corrected for e and β ($H_{EC\_ROT\_CORR}$) for the cut-grass site.

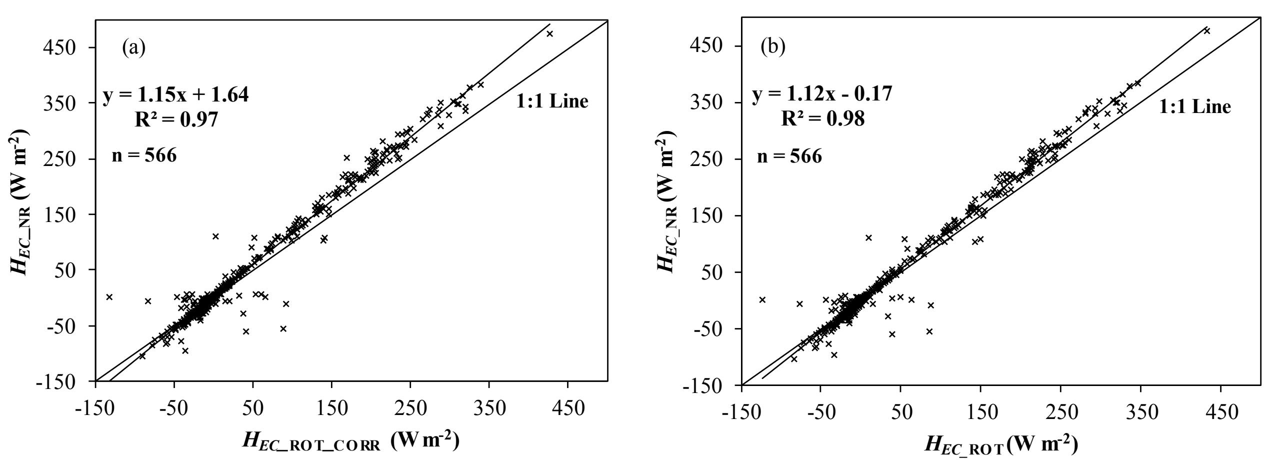

Fig. 4.6 Agreement between (a) H_{EC_NR} and $H_{EC\_ROT\_CORR}$ fluxes and (b) H_{EC_NR} and H_{EC_ROT} fluxes for the cut-grass site. Data plotted included both the stable and unstable conditions for day of year 230 to 242, 2008.

Regression comparisons for stable and unstable conditions were performed to identify the variability of the fluxes (Fig. 4.7 (a) and (b)). Stable conditions are observed when fluxes are negative while unstable conditions prevail when fluxes are positive. The stable condition plot showed much more variability in the fluxes. The R^2 was 0.68 with a slope of 0.87. Most of the points fell below a 1:1 line indicating an underestimation of the fluxes most of the time. The unstable condition fluxes performed much better with most points close to 1:1 line. The R^2 was 0.99 with a slope of 1.12. This shows that during unstable conditions, about 12% of the *H* is overestimated. Nevertheless, most studies are interested in measurements during unstable conditions especially for evaporation measurements.

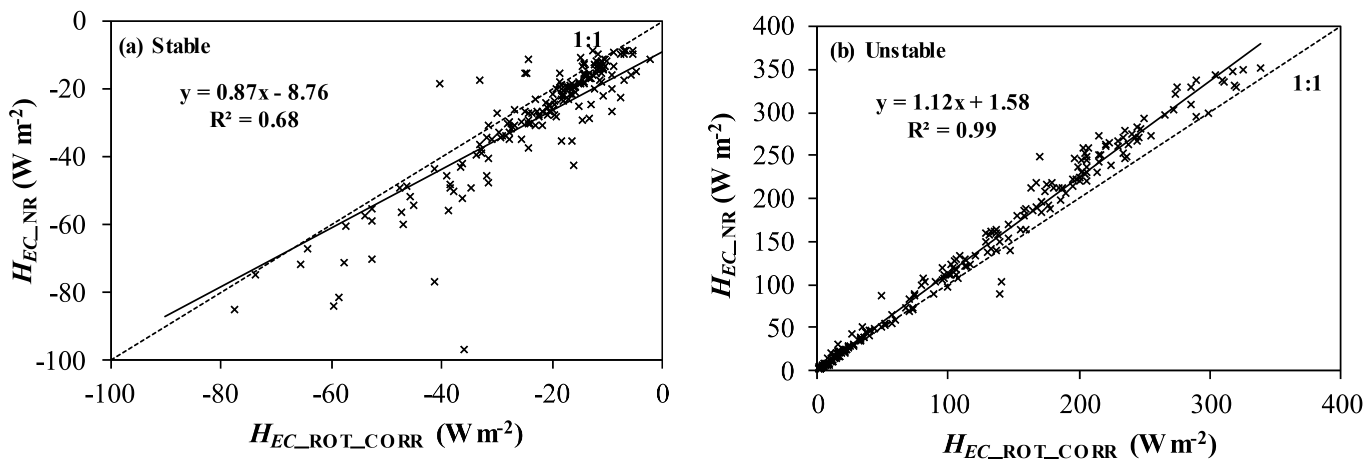

Fig. 4.7 Agreement between H_{EC_NR} and $H_{EC\_ROT\_CORR}$ fluxes for (a) stable and (b) unstable conditions for day of year 230 to 242, 2008.

Table 4.1 Statistical results obtained from comparing unrotated eddy covariance sensible heat flux (H_{EC_NR}) and rotated H_{EC} (H_{EC_ROT}) fluxes with and without correction for water vapour pressure (e) and β during both unstable and stable conditions for day of year 230 to 242.

Site	Measurement period	Measurement height (m)	Data treatment	Slope	Intercept (W m^{-2})	R^2	*n*
Cut-grass	18 to 30 Aug, 2008	2 m	H_{EC_ROT} *vs* H_{EC_NR}	1.12	-0.17	0.98	566
			$H_{EC\_ROT\_CORR}$ *vs* H_{EC_NR}	1.15	1.64	0.97	566

4.3.4 Seasonal and diurnal patterns in the energy balance components

Measurements of net irradiance R_n, sensible heat flux H_{EC}, soil heat flux G, and estimation of latent heat flux LE as a residual of the shortened energy balance, for the cut-grass site in May 2008 (DOY 143) are presented in Fig. 4.8(a). The dominant component is net irradiance followed by the sensible heat flux. The soil heat flux between 10h00 and 14h00 is greater than the computed latent heat flux. The energy balance components for the tall-grass site are illustrated in Fig. 4.8 (b). Figures 4.8 (a) and (b) show the effect of two contrasting surfaces on the energy balance components and consequently on the total evaporation ET. There was no significant variation for the other components except for the latent heat flux LE which was slightly higher for the tall-grass site.

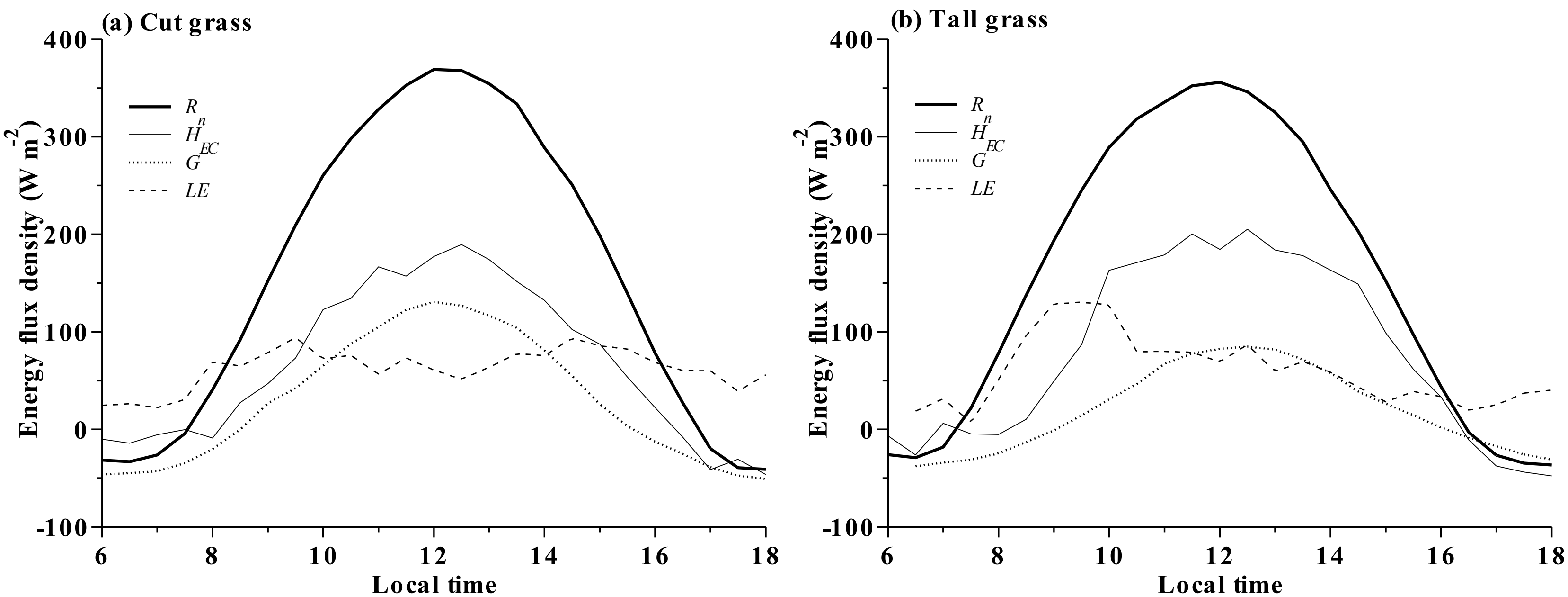

Fig. 4.8 Diurnal variation of surface energy balance components: net irradiance R_n and the sensible H_{EC}, latent LE and soil heat G fluxes for (a) the cut-grass and (b) the tall-grass sites for DOY 143 (2008).

Table 4.2 summarizes the daily energy balance fluxes (daily totals in MJ m^{-2} for unstable conditions). The available energy flux R_n–G, Bowen ratio β, excluding low values due to very cloudy conditions, daily total evaporation ET and grass reference evaporation ET_o are also tabulated. Individual energy balance fluxes varied from day to day.

Table 4.2 Daily values for May (DOY 142 to 147), June (DOY 154 to 168), and July (DOY 185 to 201) of net irradiance R_n, eddy covariance sensible heat flux (H_{EC}), latent heat flux (LE), soil heat flux (G), available energy flux (R_n - G = H_{EC} + LE), and Bowen ratio (β) for the cut-grass site. All energy balance component fluxes were computed for unstable conditions.

DOY (2008)			Energy balance components							
			R_n (MJ m^{-2})	H_{EC} (MJ m^{-2})	G (MJ m^{-2})	LE^a (MJ m^{-2})	ET^b (mm)	ET_o (mm)	R_n-G (MJ m^{-2})	β^c
	Cut grass									
142			5.34	2.04	1.51	1.78	0.73	2.02	3.82	1.14
143			7.45	3.27	1.97	2.21	0.91	2.32	5.49	1.48
144	May		7.62	3.44	1.93	2.24	0.92	2.26	5.68	1.53
145			6.48	2.86	1.72	1.90	0.78	2.08	4.77	1.51
146			7.09	3.49	1.61	1.99	0.82	1.95	5.48	1.75
147			7.21	3.39	1.79	2.04	0.84	2.16	5.42	1.66
		Total	**41.20**	**18.49**	**10.54**	**12.17**	**5.01**	**12.79**	**30.66**	
154			4.34	2.18	1.28	0.89	0.37	1.39	3.07	2.46
155			1.93	1.25	0.42	0.26	0.11	1.93	1.51	4.84
156			7.57	3.22	1.80	2.55	1.05	0.49	5.77	1.26
157			7.48	3.10	1.84	2.53	1.04	2.03	5.64	1.23
158			8.88	2.91	2.05	3.91	1.61	2.12	6.83	0.74
159	June		1.27	0.20	0.00	1.06	0.44	2.49	1.27	0.19
163			6.97	3.16	1.56	2.25	0.92	2.52	5.41	1.41
164			11.85	2.86	2.06	6.93	2.85	1.56	9.79	0.41
165			7.38	3.03	2.10	2.25	0.93	2.29	5.28	1.35
166			7.12	2.86	2.12	2.14	0.88	2.71	5.00	1.33
167			7.09	2.80	2.05	2.24	0.92	2.43	5.04	1.25
168			1.52	0.41	0.46	0.65	0.27	2.71	1.06	0.64
		Total	**41.93**	**15.12**	**10.35**	**27.71**	**11.40**	**31.58**	**25.47**	
186			5.86	2.49	1.79	1.58	0.65	2.48	4.07	1.58
187			6.49	3.50	1.77	1.22	0.50	2.05	4.72	2.87
188	July		7.85	3.83	1.94	2.08	0.85	2.55	5.91	1.84
189			7.67	3.21	2.09	2.37	0.97	2.62	5.58	1.36
190			6.38	2.52	1.88	1.98	0.82	2.75	4.50	1.27
196			1.69	0.39	0.29	1.01	0.42	2.20	1.40	0.38
		Total	**35.94**	**15.94**	**9.75**	**10.24**	**4.21**	**14.65**	**26.18**	

Superscripts *a*, *b* and *c* denotes components derived from total energy flux densities (MJ m^{-2}).

However, summations of the fluxes were more similar for selected days. For instance, in MJ m^{-2} the total daily net irradiance R_n, sensible heat flux H_{EC}, soil heat flux G and latent heat flux LE for May 2008 (DOY 142 to 147) were 41.20, 18.49, 10.54 and 12.17 MJ m^{-2}, respectively.

The total evaporation and grass reference evaporation over this five-day period were 5.01 and 12.79 mm, respectively. The total available energy was 30.66 MJ m^{-2}. The average Bowen ratio β was 1.51. Similar results were obtained for June 2008 (DOY 186 to 196). Substantial differences were prevalent for H_{EC} and LE. From May to June, H_{EC} slightly decreased in magnitude. There was a positive correlation between the progressive growth of the grass and ET increment. This may be due to the increased leaf area index (not measured but casual observations made) resulting from an increased total evaporation rate. Also more solar irradiance became available as the season changed from winter to spring.

4.4 Conclusions

The cut-grass site maintained low soil water content compared to the tall-grass site. The soil temperature recorded at the cut-grass site was consistently higher than that of the tall-grass site.

Sensible heat flux EC data for the cut-grass site from day of year 232 to 233 were rotated and were compared to unrotated H_{EC} fluxes. There were no significant differences between the rotated and unrotated H_{EC} fluxes. The rotated H fluxes were then corrected for water vapour pressure (e) and β. Correcting H for e and β decreased the H_{EC} by 15% for unstable conditions.

Regression comparisons of unrotated sensible heat flux H_{EC_NR} and rotated and corrected sensible heat flux $H_{EC\_ROT\_CORR}$ showed more variability for stable atmospheric conditions (slope = 0.87 and R^2 = 0.68) than for unstable conditions. The agreement between H_{EC_NR} and $H_{EC\_ROT\_CORR}$ was much improved for unstable conditions (slope = 1.12 and R^2 = 0.99).

The energy balance components for the cut-grass site showed a similar trend (diurnal variation) from day to day. The dominant component was net irradiance followed by the sensible heat flux. Soil heat flux was usually greater than the latent energy flux. As the plants at the cut-grass site recovered and started to grow new shoots, the increase of total evaporation and consequent decrease in soil heat flux became evident.

Chapter 5: Influence of fire on radiation and energy balances of a tall grassland

5.1 Introduction

Grassland ecosystems play a vital role in our lives in many ways. For example, both natural and cultivated pastures are harvested for building purposes and used to feed domestic and wild animals (Edwards and Tainton, 1990). There are several outputs from grassland ecosystems that benefit us and these may be measured in units of meat, milk, wool or cash (Pearson and Ison, 1997). Harrington *et al*. (1984) describe grasslands as semi-natural ecosystems in which we seek to get a productive output by simply adding domesticated grazing animals. The management of grasslands involve animal grazing, mowing, fire and fertilization (Dillon, 1980; Wright and Bailey, 1982; Harrington *et al*., 1984; Pearson and Ison, 1997) and irrigation (Edwards and Tainton, 1990). Each of these management practises has unique merits and demerits. For instance, overgrazing as a result of overstocking may cause soil erosion. Allowing animals to graze on burnt patches can also accelerate the independent effects of fire and grazing on soil properties (Vermeire *et al*., 2005). Similarly, burning kills both vegetation and animals in its path leaving behind an unprotected soil surface that is susceptible to the effects of soil erosion (Hodgkinson *et al*., 1984). However, for some plant species the crown and roots survive to generate new tillers in spring. Prescribed burning has been described as "the deliberate ignition of vegetation and the subsequent control of the limits of spread of the fire to achieve a desired management objective" (Hodgkinson *et al*., 1984). Burning as a management tool is necessary to increase the number of grass species due to removal of litter thereby increasing the availability of solar irradiance to the soil and plants (Fynn *et al*., 2004). Furthermore, implementation of fire as a management tool helps to release seeds from fruits, enhancing germination of hard seeds (Pearson and Ison, 1997). It has been shown that grass species richness decreased significantly in the absence of mowing or burning (Fynn *et al*., 2004). Moreover, burning is believed to disinfect grasslands of ticks and also suppresses the encroachment of unwanted plant species in grassland ecosystems (Oluwole *et al*., 2008). According to Hodgkinson *et al*. (1984), the main reasons for the implementation of fire as a management tool in pastoral lands are: control of woody plants, stimulation of herbage growth, and reduction of fire hazards due to accidental fire outbreak. Conversely, in conservation places, the main objective of using fire as a management tool is to maintain ecological diversity (Edwards, 1984).

Although management practices of grasslands are a common practice globally, they may influence surface radiation and energy balances from a landscape surface (Savage, 1981; Bremer and Ham, 1999). The surface radiation and energy balance may be altered fairly easily by altering the fraction of solar irradiance reflected by a surface. This fraction is termed the surface reflection coefficient r. In addition to anthropogenic factors such as burning (Savage and Vermeulen, 1983) and mowing (Fynn *et al*., 2004), natural factors such as diurnal and seasonal patterns can alter the surface reflection coefficient (Wang and Davidson, 2007). For example, spring burn of tall grassland caused large variations in the surface reflection coefficient which resulted in differences in the energy balance between burnt and unburnt areas (Bremer and Ham, 1999). Additionally, Bremer and Ham (1999) reported that spring burning of a tallgrass prairie had significant effects on fluxes of water and energy. In their study, the application of fire to a grassland area modified the microclimate of the surface and resulted in a larger canopy and increased latent heat fluxes *LE* than on unburnt grassland. The duration of fire for a prescribed burning might last for a few minutes, but the above-ground biomass is completely destroyed and the nutrients are completely volatilized (Harrington *et al*., 1984). Some of the effects of fire are: changes in infiltration, total evaporation, rainfall interception, and soil water repellence. All these changes may directly or indirectly affect the soil water content as well as soil temperature dynamics (Vermeire *et al*., 2005).

The net irradiance R_n, solar irradiance I_s, reflected solar irradiance rI_s and infrared irradiances (L_u and L_d) are some of the most important measurements for most micrometeorological applications (Campbell and Diak, 2005). The net infrared irradiance is given by the difference between outgoing L_u and downward L_d infrared irradiances. Several types of radiometers can be used to obtain each or a combination of the components of the surface radiation balance. The CNR1 four-component net radiometer, with pyranometers and pyrgeometers facing up and down, provides individual measurements of the four radiant energy components that make up the net irradiance. The net irradiance R_n is computed as the difference between the incoming and outgoing energy components (Eq. 5.1).

The surface radiation balance of a flat and extensive surface is given by:

$$R_n = I_s - r\,I_s - L_u + L_d \qquad (5.1)$$

where the net irradiance R_n, is the difference between the incident solar irradiance I_s and the reflected solar irradiance rI_s and the net infrared irradiance ($-L_u + L_d$).

The shortened surface energy balance of a flat and extensive surface is given by:

$$R_n = H + LE + G \tag{5.2}$$

where H, LE and G are the sensible, latent energy and soil heat fluxes, respectively.

The partitioning of the available energy flux $R_n - G$ into sensible H and latent LE heat fluxes is often expressed through the Bowen ratio $\beta = H/LE$.

Fire has many implications for the radiation and energy balance of grasslands. The objective of this study is to investigate the impacts of fire on radiation and energy balance components.

5.2 Materials and methods

5.2.1 Study area

The burning experiment was conducted at Ukulinga (30^{o} 40′E, 29^{o} 67′S), the research and training farm of the University of KwaZulu-Natal, Pietermaritzburg, South Africa. The experiment was located on a relatively flat grassland area with an elevation of 840 m above sea level. The lithology of the area consists of Ecca group shales of Karoo sedimentary sequence and the soil type is mainly Bonheim (Dillon, 1980; Fynn *et al*., 2004). A detailed account of climate and vegetation of this area is described in Chapter 3.

5.2.2 Experimental design

The experiment was carried out between March and December 2008. Initially, the cut-grass site was mowed while the tall-grass site remained intact until the burn (11 July 2008). A CNR1 (Kipp and Zonen, Delft, The Netherlands) four-component net radiometer was placed at 2 m above soil surface at the tall-grass site two days before burning. It was then removed from the site before the fire was started (Fig. 5.1 (a)).

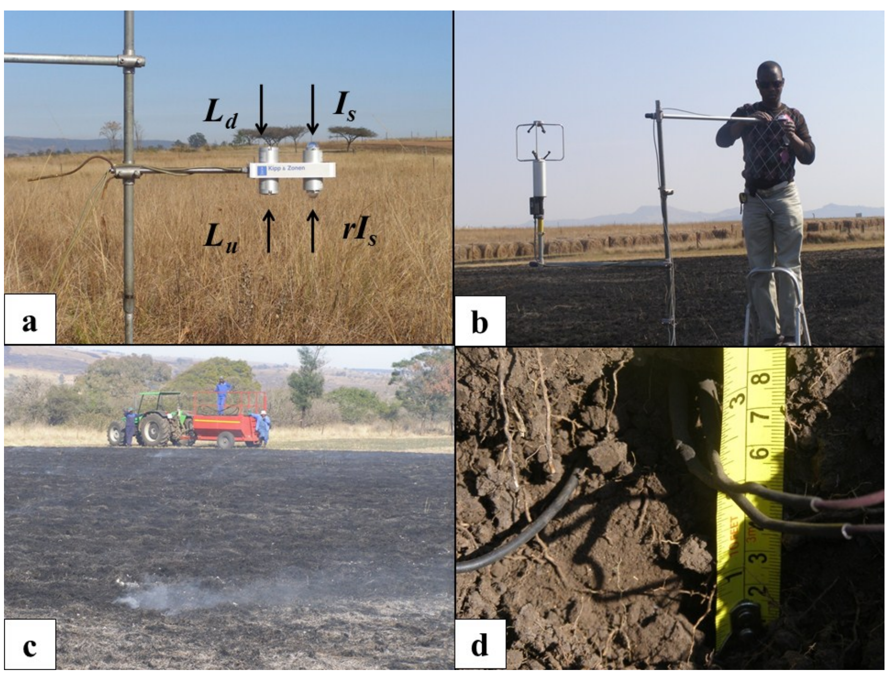

Fig. 5.1 (a) The CNR1 net radiometer set up above the tall-grass site before burning; (b) the three-dimensional sonic anemometer and net radiometer set up two hours after the burn; (c) University support staff control the extent of the fire; and (d) the installation of soil heat flux plates and soil averaging thermocouples after the burn.

The net radiometer was installed again above the burnt grass after the fire has died. All other energy balance equipment was set up as described in Chapter 3. Soil samples were taken randomly from the cut-grass site and the now burnt grass site after the first spring rains. The samples were taken at a depth of 0 to 150 mm and were analysed for C: N: S and texture. The soil analysis results showed that the soil from the experimental field contained less than 30% organic content and hence should be classified as a mineral soil. This information was required for the ThetaProbe soil water content calculations.

5.3 Results and discussion

5.3.1 Radiation balance components

The diurnal variation of the surface radiation balance components for DOY 194 before the burn is shown in Fig. 5.2 (a). The surface reflection coefficient r showed a slight variation throughout the day with a value of 0.16 recorded at noon when the solar irradiance I_s was 636.10 W m^{-2}. The reflected solar irradiance ranged between 0 and 100 W m^{-2} for DOY 194. The net irradiance R_n followed a similar trend to I_s with a noon value of 534.6 W m^{-2}. As expected the infrared energy components (L_u and L_d) were both generally low compared to the I_s and R_n. The downward infrared radiation L_d showed a significant decrease between sunrise and sunset while the outgoing infrared radiation showed a similar trend as the I_s and R_n. The maximum L_u and L_d values recorded at noon were 430.1 and 286.3 W m^{-2}, respectively.

The diurnal variation of the surface radiation balance components for DOY 197, three days after the burn, is illustrated in Fig. 5.2 (b). The uneven nature of the solar irradiance I_s and net irradiance R_n curves is due to cloud cover. The surface reflection coefficient r was more uniform after the burn but very small with a value of 0.01 as compared to that on DOY 194 before the burn that had a value of 0.16. The reflected solar irradiance rI_s was very small in magnitude (0 to 9.5 W m^{-2}) when compared to DOY 194 and this may be due to the cloudy conditions that prevailed on DOY 197. The outgoing infrared irradiance changed uniformly with relation to the sun's position in the sky. The downward infrared irradiance was significantly influenced by the cloud cover, for partial clear sky L_d decreased significantly and when it became overcast, L_d showed a linear increase. This is because clouds play a major role in preventing the escape of the infrared irradiance by reflecting it back to the Earth's surface. The maximum L_u and L_d values recorded at noon for DOY 197 were 372.1 and 437.5 W m^{-2}, respectively. All the surface radiation balance components showed consistence at the burned site (Fig. 5.3).

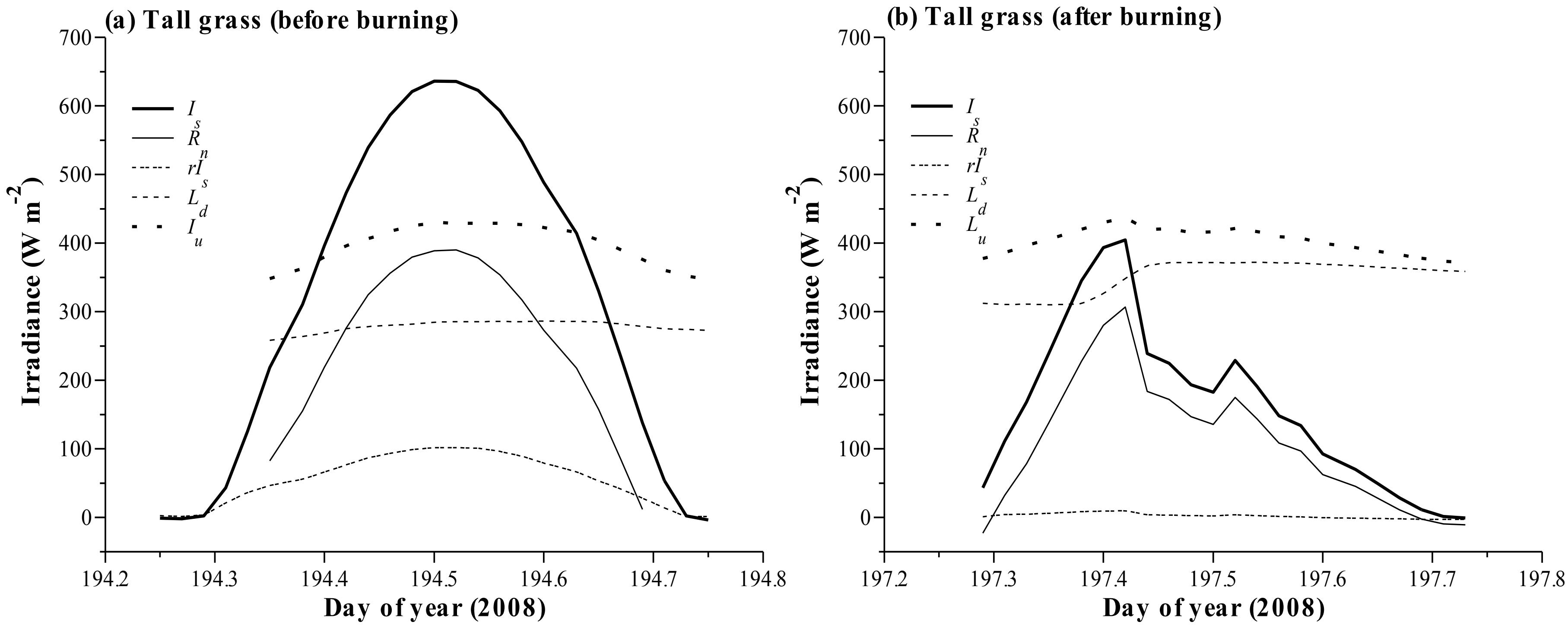

Fig. 5.2 (a) and (b) Diurnal variation of the surface radiation balance components: net irradiance R_n, total solar irradiance I_s, reflected solar irradiance rI_s, downward infrared L_d, and outgoing infrared L_u radiation for DOY 194 a day before the burn of a tall grassland and for DOY 197, two days after the burn respectively.

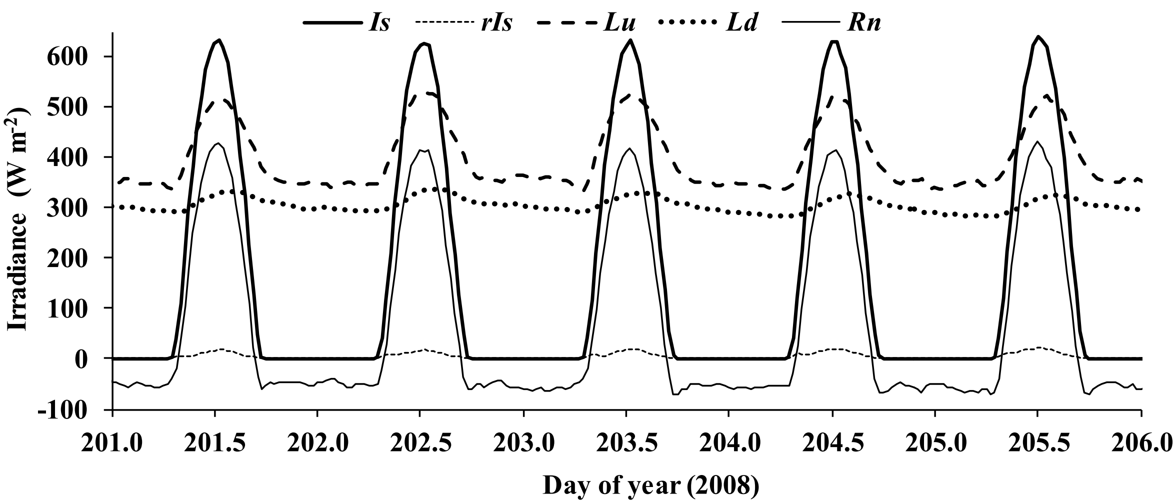

Fig. 5.3 Diurnal variation of the surface radiation balance components: net irradiance R_n, total solar irradiance I_s, reflected solar irradiance rI_s, downward infrared L_d, and outgoing infrared L_u irradiance from DOY 201 to 205 after the burn of the tall grassland.

Surface reflection coefficient r depends on the properties of the surface, and changes diurnally and seasonally. Surface reflection coefficient was determined at the tall-grass site before and after the burn of the plants. Figure 5.4 shows surface reflection coefficient for day of year 193 before burning and 4 days after burning (DOY 197). The grass height at the tall-grass site before burning was 0.4 m, with a dry surface litter that completely covered the soil. The surface reflection coefficient for the tall-grass site was monitored on DOY 193 from 08h00 to 17h00 (local time). The reflection coefficient was found to be high in the morning with a decreasing trend towards noon then starts to increase again towards sunset. The average surface reflection coefficient recorded for the tall-grass site before (DOY 193, 2008) and after burn (DOY 197, 2008) was 0.166 and 0.018 respectively. The surface reflection coefficient observed for the study site before and after burning compares well with results reported by Savage and Vermeulen (1983).

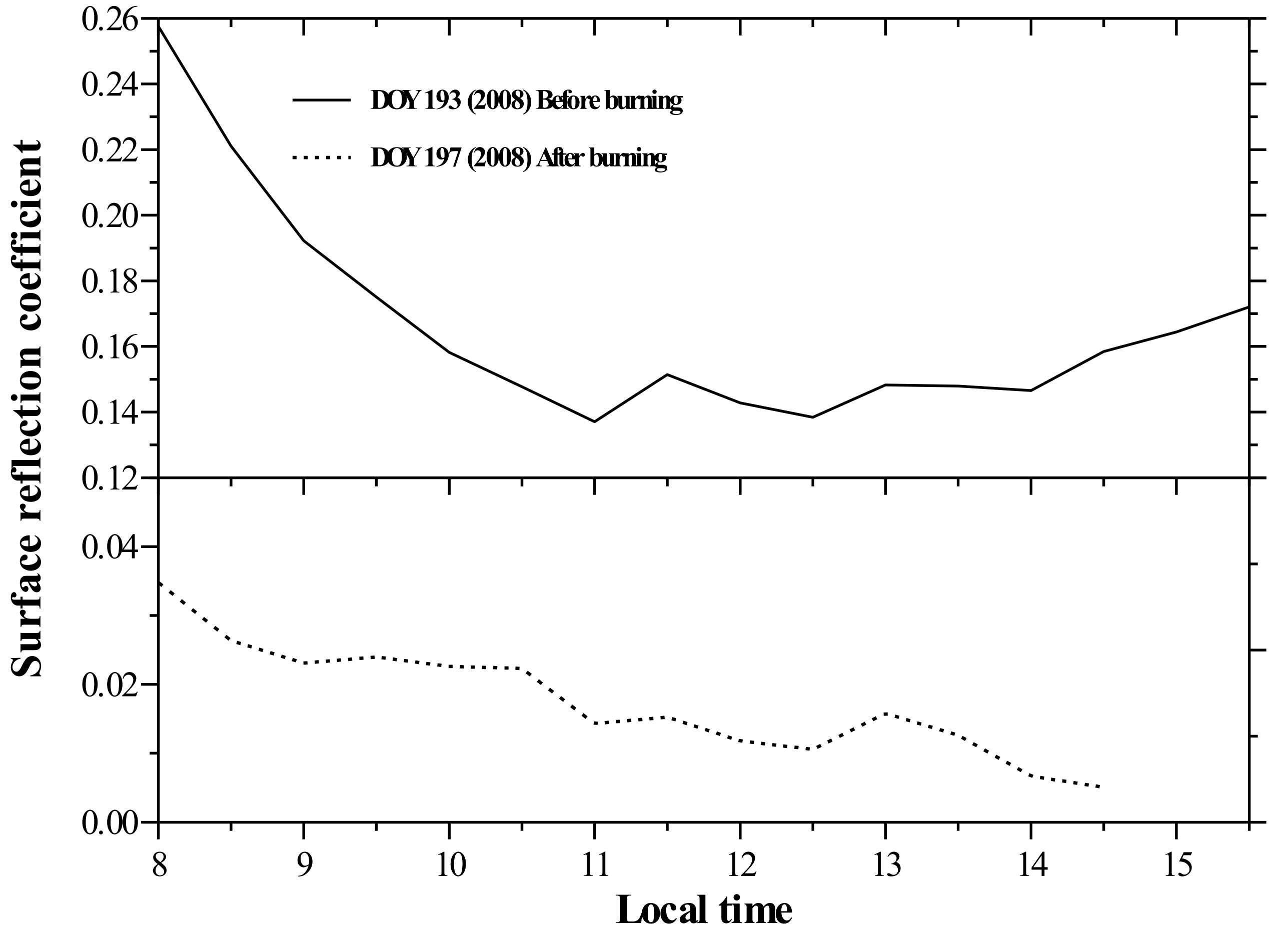

Fig. 5.4 Diurnal variation of surface reflection coefficient *r* for the tall-grass site before the burn (DOY193) and after the burn (DOY 197).

5.3.2 Soil water content

Burning of grasslands removes the litter and plants that cover the soil surface, thereby changing the surface properties of burnt surfaces in various ways. The effects of burning on soil water content have been investigated previously (Bremer and Ham, 1999; Vermeire *et al*., 2005). As a result of the burn, the soil water content decreased from about 0.277 m^3 m^{-3} before the burn to 0.239 m^3 m^{-3} immediately after the burn (Fig. 5.5). The tall-grass site maintained higher soil water content compared to after burning due to the litter layer and due to plants providing shade to the soil resulting in reduced soil water loss by evaporation. Furthermore, burning of the above-ground litter resulted in a darkened bare soil surface resulting in increased net irradiance and increased soil water loss.

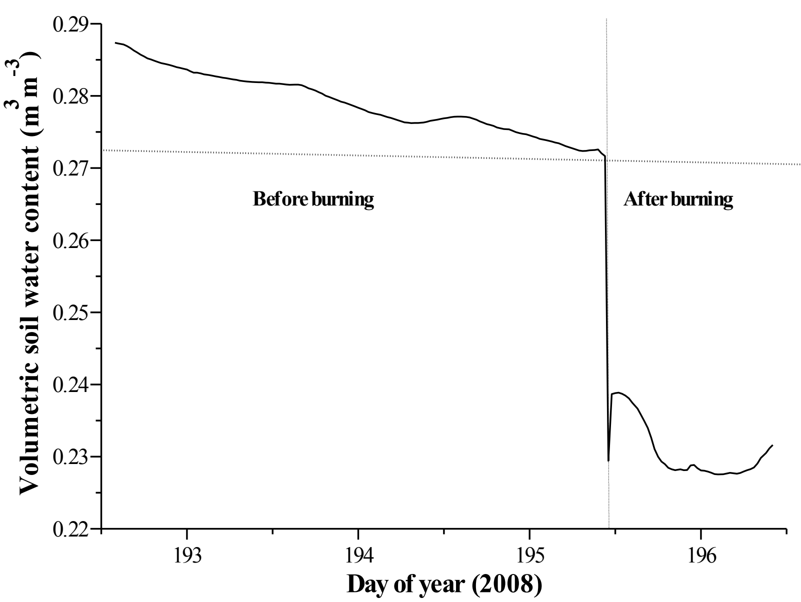

Fig. 5.5 Variation of soil water content at a depth of 100 mm before and after burning of the tall-grass site.

5.3.3 Soil temperature

On average, daily soil temperature at 0.08 m was 2.0 ^{o}C greater in the burnt site towards the end of the winter season compared to the tall-grass site. The removal of the dead biomass and standing grass by burning is likely to have contributed to increase in soil temperature due to the increased solar irradiance at the soil surface. Bremer and Ham (1999) reported an average soil temperature increase of 3.9 ^{o}C at 25 mm for their burnt site. This value was greater than that of the tall-grass site after burning probably due to the difference in seasons, soil type or elevation.

5.3.4 Diurnal and seasonal patterns in energy balance components

The various energy balance terms were integrated over the whole day (with a filter to remove values corresponding to stable conditions, usually negative night time values) for different days for the tall-grass site before burning and after burning. Data from the onset of the burn of the tall-grass site are presented to illustrate the effects of the burn on the energy balance components at various stages of grass growth. Before the burn R_n was generally low compared to the values recorded after the burn. The energy flux densities for R_n, LE, H_{EC} and G before and after the burn are illustrated (Figs 5.6 and 5.7). For example, on DOY 164, the total R_n before burning was 6.78 MJ m^{-2} compared to 8.48 MJ m^{-2} for DOY 199 after the burn (Table 5.1).

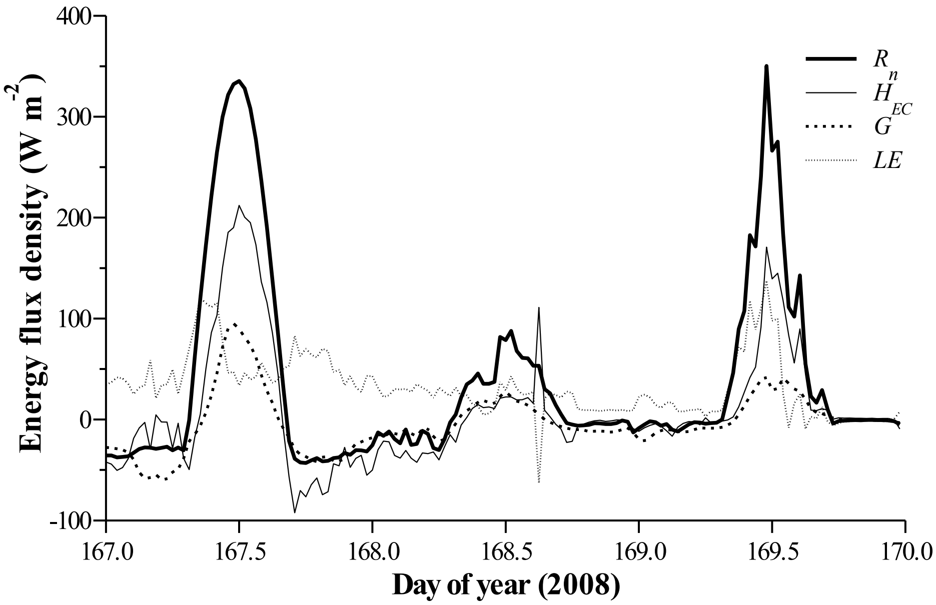

Fig. 5.6 Diurnal patterns on DOY 167 to 169 (before the burn) of net irradiance R_n, latent energy flux LE, sensible heat flux H_{EC}, and soil heat flux G for the tall-grass site before the burn.

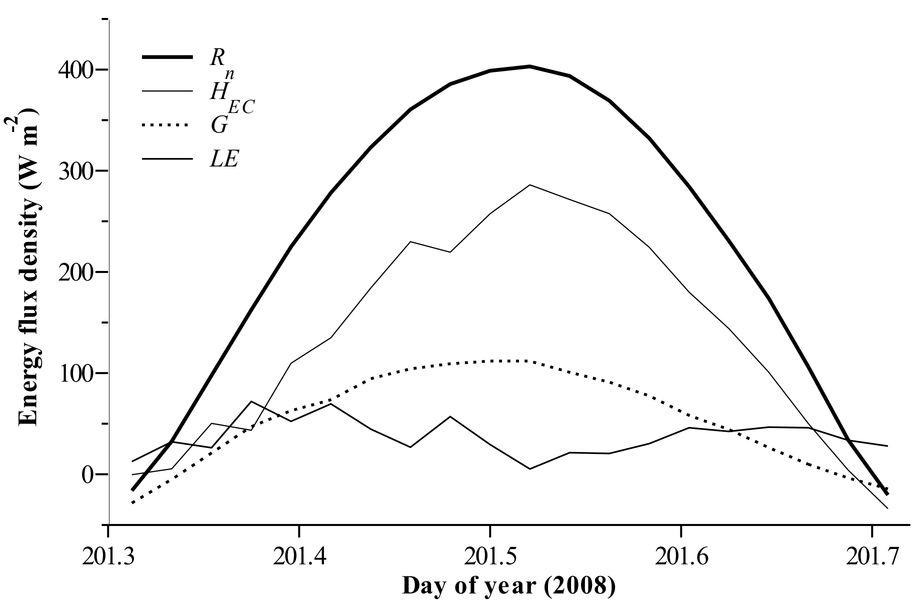

Fig. 5.7 Diurnal patterns on DOY 201 (after the burn) of net irradiance R_n, latent energy flux LE, sensible heat flux H_{EC}, and soil heat flux G for the tall-grass site 6 days after the burn.

Table 5.1 Daily values for June (DOY 164 to 169) and July (DOY 197 to 202) of net irradiance (R_n), eddy covariance sensible heat flux (H_{EC}), latent energy flux (LE), total evaporation (ET), grass reference evaporation (ET_o) soil heat flux (G), available energy flux ($R_n - G$) and Bowen ratio (β). Values of R_n, H_{EC}, LE, and G are for the period 06h00 to 18h00.

DOY (2008)										
			Energy balance components							
			R_n (MJ m^{-2})	H_{EC} (MJ m^{-2})	G (MJ m^{-2})	LE^a (MJ m^{-2})	ET^b (mm)	ET_o (mm)	R_n - G (MJ m^{-2})	β^c
	Unburnt									
164			6.78	3.45	1.32	2.01	0.83	1.56	5.46	1.71
165			6.84	3.53	1.47	1.84	0.76	2.29	5.37	1.92
166	June		6.77	3.60	1.42	1.75	0.72	2.71	5.35	2.05
167			6.70	3.49	1.31	1.90	0.78	2.43	5.39	1.84
168			1.57	0.59	0.42	0.57	0.23	2.71	1.16	1.04
169			4.37	2.03	0.71	1.63	0.67	0.30	3.65	1.24
		Total	**33.03**	**16.68**	**6.65**	**9.70**	**3.99**	**11.99**	**26.38**	
	Burnt									
197			4.12	2.59	0.90	0.63	0.26	2.93	3.22	4.14
198			3.01	1.87	0.78	0.36	0.15	1.42	2.23	5.14
199	July		8.48	4.42	2.21	1.85	0.76	0.80	6.27	2.39
200			7.70	4.46	2.06	1.18	0.49	2.19	5.65	3.77
201			8.26	4.97	2.06	1.23	0.51	2.40	6.20	4.04
202			8.07	4.61	2.15	1.31	0.54	2.46	5.92	3.53
		Total	**39.65**	**22.92**	**10.17**	**6.56**	**2.70**	**2.80**	**29.48**	

Superscripts *a*, *b* and *c* denotes components derived from total energy flux densities (MJ m^{-2}).

A similar trend was observed for daily values of H_{EC} and G but LE values were greatly reduced following the burn. For example, the total of LE (MJ m^{-2}) for DOY 164 to 169 (before the burn) was 9.70 MJ m^{-2} compared to 6.56 MJ m^{-2} for DOY 197 to 202 (after the burn). Energy fluxes on DOY 169 were representative of the period before the burn, when the effect of the above ground litter was dominant. The high R_n values observed following the burn were due to the reduced surface reflection coefficient as a result there was increased energy available for heating the soil and evaporating more water from the soil. Conversely, the tall-grass site showed relatively low R_n values as most of the radiant energy was absorbed by the dead biomass and then lost to the atmosphere as sensible heat. Savage and Vermeulen (1983) and Bremer and Ham (1999) have reported similar trends from their experiments carried out at Ukulinga, Pietermaritzburg, South Africa and Manhattan, Kansas, USA, respectively.

The daily total evaporation varied from day to day depending mainly on net irradiance R_n. For example, DOY 164 to 167 had an average ET of 0.67 mm and ET_o of 2.00 mm before the burn and for DOY 197 to 202, a value of 2.00 mm and 2.03 mm were recorded, respectively. Consequently, ET accumulation from DOY 164 to 169 was 3.99 mm before the burn compared to 2.70 mm for the days 197 to 202 after the burn. The high rate of evaporation for the tall-grass site may be attributed to the combined water loss from the soil surface, intercepted water by the above ground biomass and transpiration from the standing grass. Conversely, the evaporation rate declined after the burn due to the drastically reduced leaf area rendering the measured total evaporation to be exclusively from the soil. Although, the daily evaporation averages varied slightly from day to day, in step with the net irradiance, there was a general increase in total evaporation as the grass started to re-grow. The grass reference evaporation remained consistently high for the entire experimental period. The Bowen ratio (β) values reported in Table 5.1 were computed from the daily total values of H_{EC} and LE (MJ m^{-2}). The β values also varied diurnally with low evaporation rates corresponding to high β values and vice versa.

5.4 Conclusions

Burning towards the end of winter had a significant impact on the radiation and energy balances of the grassland surface. Removal of dead litter above-ground by fire changed the optical properties of the tall-grass site, causing a significant decrease in the surface reflection coefficient. Consequently, soil temperature increased following burning due to increased solar irradiance interception at the soil surface. The fluxes R_n, H_{EC} and G also increased after the burn but the LE component decreased since the grass leaf area was drastically reduced thereby significantly reducing transpiration. The decrease in the rate of evaporation after the burn explains the significance of the grassland communities in their contribution to the hydrologic cycle. There was a dramatic change in soil water content 30 minutes after the burn which later recovered. After the first rains of spring, green patches of grass leaves became more visible and the growing canopy had begun to shade the soil surface of the burnt site. This caused changes in the reflection coefficient and available energy flux. The reflection coefficient r and reflected solar irradiance rI_s progressively increased after the burn. The daily total evaporation ET and grass reference evaporation ET_o also increased as the grass continued to grow and cover most of the soil surface.

In summary, the results of this study have shown that land management strategies such as burning can significantly affect the surface radiation and energy balance of grasslands through the change in net irradiance. Burning effectively decreases the reflection coefficient, reflected solar irradiance and soil water content and increases the soil temperature causing changes in all of the energy balance components due to the removal of litter and changes in canopy structure. The consideration of all of these changes is vital when predicting climate change and water budgets of grassland communities over large areas.

Chapter 6: Application of the surface renewal method for estimating sensible heat flux

6.1 Introduction

Surface renewal sensible heat flux H_{SR} was estimated using a simplified SR analysis model. The simplified model used a/τ (^{o}C s^{-1}) for the average rate of change in air temperature for the total ramp period:

$$H_{SR} = \alpha \rho c_p \frac{a}{\tau} z \qquad (6.1)$$

where α is the SR weighting factor, ρ the air density (kg m^{-3}), c_p the specific heat capacity of air at constant pressure (J kg^{-1} K^{-1}), a amplitude (^{o}C), τ the total ramp duration corresponding to the inverse ramp frequency of the air temperature ramps (s) and z the measurement height (m). The total ramp period is calculated from:

$$\tau = L_r + L_q \qquad (6.2)$$

where L_r is the ramp period and L_q the quiescent period or undisturbed temperature period (Antonia *et al*., 1982).

The structure functions of air temperature and the analysis technique of Van Atta (1977) are then used to estimate the amplitude a and τ the ramp period (Eq. (6.2)). The structure function value $S^n(r)$ is usually calculated for each averaging period (2- and 30-min), from high-frequency air-temperature measurements at frequency f using the relation in Eq. (2.20). The Van Atta (1977) method estimates the mean value for amplitude a during the time interval by solving the following equation for real roots (Mengistu and Savage, 2010a):

$$a^3 + pa + q = 0 \tag{6.3}$$

where:

$$p = 10S^2(r) - \frac{S^5(r)}{S^3(r)} \tag{6.4}$$

and

$$q = 10S^3(r) \tag{6.5}$$

The ramp period τ is calculated using:

$$\tau = -\frac{a^3(r)}{S^3(r)} \tag{6.6}$$

The structure-function theory requires that the ramp period τ be less than the lag time r for the theory to hold else it will be in valid. Typical τ values (τ > 10 r) have been suggested by Van

Atta (1997). The SR spreadsheet iteration method (Savage, 2010a) uses the condition that $\tau > 5\ r$ with an upper limit for τ of 600 s. The iteration method involves Eq. (6.1) and (6.3) to estimate H_{SR}. The measurements of second-, third- and fifth-order temperature structure functions (Eq. (6.4) to (6.6)) are calculated online. To do the iteration to solve for a, the calculation starts from zero upwards in steps of 0.005 for unstable conditions. This value of a is used in Eq. (6.3) and if the result is less than 0.01, H_{SR} is computed with $\alpha = 1$. If the result of Eq. (6.3) is greater than 0.01, a is incremented by 0.005 and the process repeated. If no root for Eq. (6.3) is found, no estimate for H_{SR} is calculated. After H_{SR} calculations in Excel, careful data sorting is required before fluxes can be statistically compared with EC method fluxes to remove blank data.

6.2 Calibration and validation of SR method

A short-term comparison of EC and SR methods was carried out at the cut grass experimental site. SR estimates of H were obtained using an iterative procedure in Excel (Savage, 2010b). Turbulence fluxes for unstable conditions were used for calibration and validation of the H_{SR} fluxes using different data sets. The calibration step involved obtaining the SR weighting factor α for different fine-wire thermocouple heights and different lag times. The second step involved validating the SR method by applying the α value to H_{SR} fluxes and performing H_{SR} versus H_{EC} plots. During the calibration period, the vegetation height at the cut-grass site was 0.2 m. The SR weighting factor α was obtained for each height and lag time r by calibration by plotting H_{EC} *vs* H_{SR} uncorrected for α (α is the slope of the linear fit through the origin) (Fig. 6.1). The SR thermocouple at 0.7 m above soil surface and r = 0.4 and 0.8 s yielded the highest α values, 1.90 and 2.26, respectively. However, reasonable α of values of 0.71 and 1.01 where obtained for a fine-wire thermocouple at 1.2 m above soil surface and r = 0.4 and 0.8 s, respectively. These α values were then used to validate the H_{SR} data computed iteratively in Excel for a different data set. The validation procedure, for unstable conditions, involved plotting graphs of 30-min surface renewal (H_{SR}) versus corrected eddy covariance (H_{EC}) (Fig. 6.2).

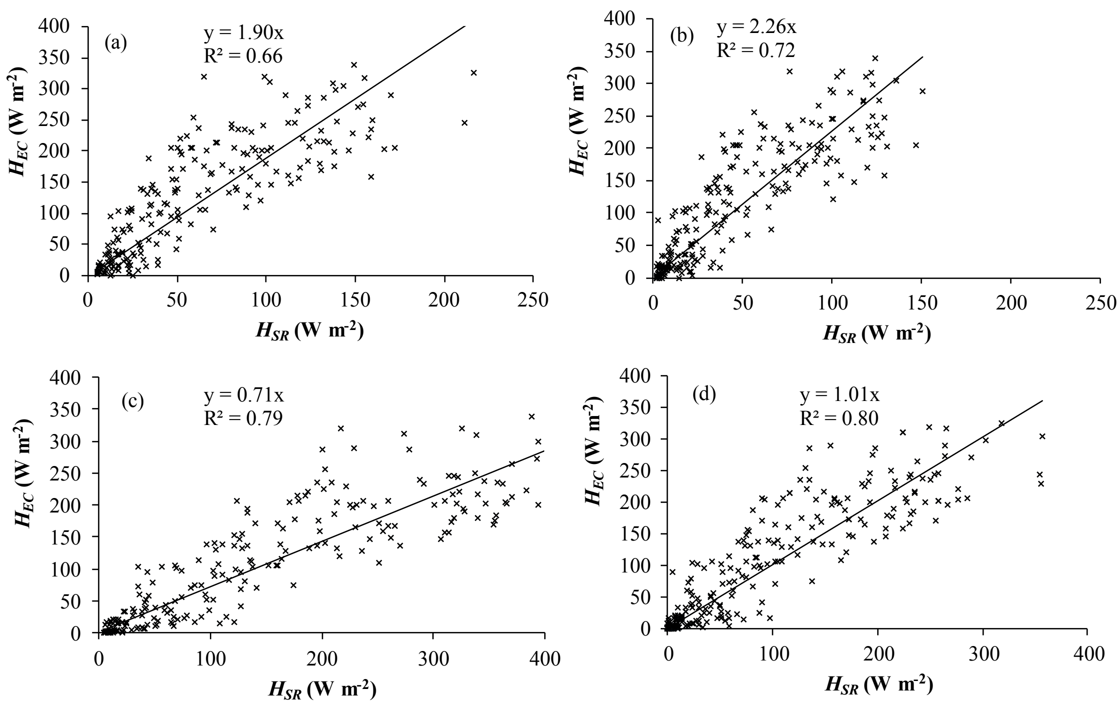

Fig. 6.1 Calibration plots for the SR method using half-hourly corrected eddy covariance (H_{EC}) versus surface renewal (H_{SR}) estimates of sensible heat flux uncorrected for α for day of year 223 to 242 (2008) during unstable conditions: (a) H_{EC} *vs* H_{SR} at 0.7 m above ground and time lag (r = 0.4 s); (b) H_{EC} *vs* H_{SR} at 0.7 m above ground and time lag (r = 0.8 s); (c) H_{EC} *vs* H_{SR} at 1.2 m above ground and lag time (r = 0.4 s) and (d) H_{EC} *vs* H_{SR} at 1.2 m above ground and lag time (r = 0.8 s) *vs* H_{EC}.

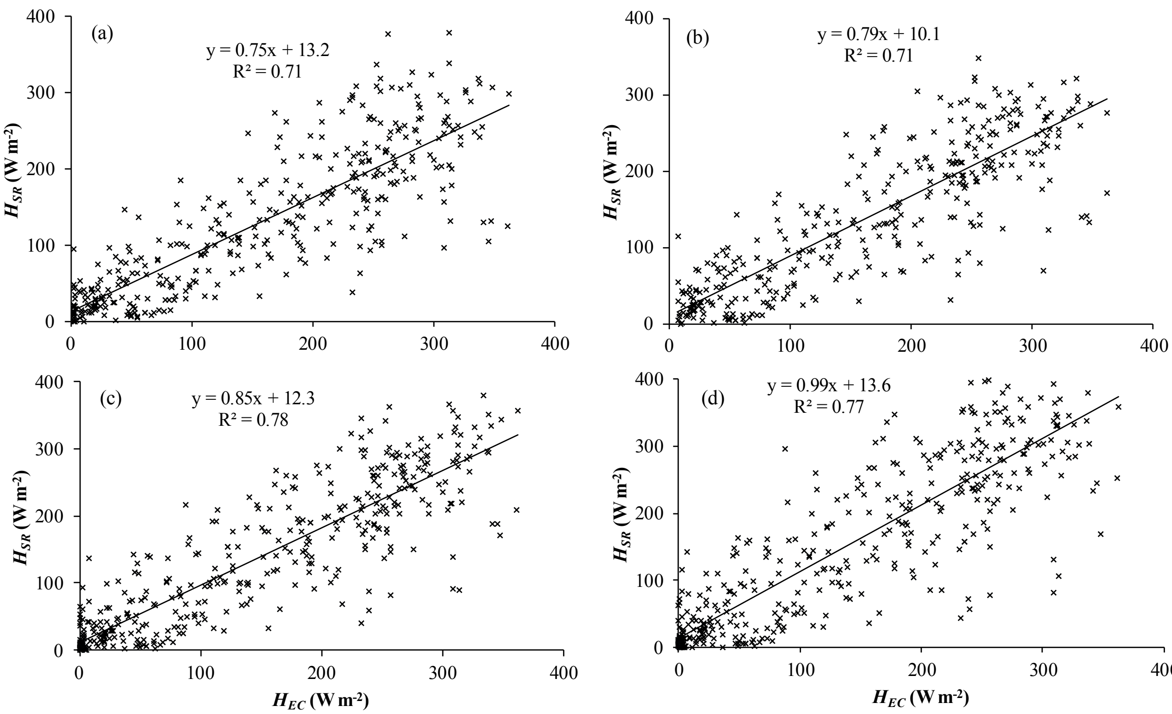

Fig. 6.2 Validation plots for the SR method using half-hourly measurements using surface renewal (H_{SR}) versus corrected eddy covariance sensible heat flux (H_{EC}) for day of year 243 to 262 (2008) during unstable conditions: (a) H_{SR} at 0.7 m above ground and time lag 0.4 s *vs* H_{EC} ($\alpha = 1.96$); (b) H_{SR} at 0.7 m above ground and time lag ($r = 0.8$ s) *vs* H_{EC} ($\alpha = 2.26$); (c) H_{SR} at 1.2 m above ground and lag time ($r = 0.4$ s) *vs* H_{EC} ($\alpha = 0.71$) and (d) H_{SR} at 1.2 m above ground and lag time 0.8 s *vs* H_{EC} ($\alpha = 1.01$).

Regression of H_{SR} versus H_{EC} for the calibration period was performed and for $z = 0.7$ m and both lag times 0.4 and 0.8 s, yielded an R^2 of 0.71 (Fig. 6.1(a) and (b)). This height (0.7 m) had the highest α value for both lag times (1.90 and 2.26), greater than that reported by Mengistu (2008). It is possible the SR fine-wire thermocouples at $z = 0.7$ m above soil surface accumulated dirt more than the ones at 1.2 m, impacting on the high frequency air temperature measurements at the site.

Nevertheless, better agreement was obtained for z = 1.2 m and lag times of 0.4 and 0.8 s. Lag times 0.4 and 0.8 s for z =1.2 m yielded an R^2 of 0.78 and 0.77, respectively. For r = 0.4 s, H was under-estimated by 22% while for r = 0.8 s the under-estimation was 33% (Fig. 6.2 (c) and (d)). Detailed regression results for the calibration data are presented in Table 6.1.

6.2 SR and EC comparisons

The energy balance components were computed for unstable conditions for day of year 246, 2008. The pattern of the surface energy fluxes responded to the prevailing weather conditions. The calibrated surface renewal sensible heat H_{SR} and latent energy fluxes LE_{SR} were computed for measurement height (z) 1.2 m above soil surface and lag times 0.4 and 0.8 s and compared to eddy covariance sensible heat H_{EC} and latent energy flux H_{EC} (Fig. 6.3). Generally, H_{SR} exceeded H_{EC} before noon but was less than the H_{EC} in the afternoon for a measurement height 1.2 m and both lag times. The differences between H_{SR} and H_{EC} were greater in magnitude for the 0.8 s lag time.

Table 6.1 Regression statistics obtained by validating the SR method against the EC method using plots of 30-min H_{SR} versus H_{EC} for day of year 243 to 262 (2008), for unstable conditions. The SR weighting factor (α) is the slope of the linear fit through the origin and was obtained during the calibration period.

z, above soil surface (m)	**Lag time (s)**	**Slope**	**Intercept ($W\ m^{-2}$)**	**R^2**	***n***	**Weighting factor (α)**
0.7	0.4	0.75	13.21	0.71	375	1.96
0.7	0.8	0.77	10.10	0.71	352	2.26
1.2	0.4	0.85	13.30	0.78	427	0.71
1.2	0.8	0.99	13.64	0.77	435	1.01

The fluxes LE_{SR} and LE_{EC} were both computed as a residual from the shortened energy balance equation. The agreement between LE_{SR} and LE_{EC} was reasonable for most of the day with LE_{EC} generally larger than LE_{SR} before noon (DOY 246, 2008). The calculated total evaporation for surface renewal ET_{SR} was greater than that of eddy covariance ET_{EC}, 1.67 mm and 1.57 mm, respectively (Fig. 6.3 (a)).

Generally, for the measurement height (z) of 1.2 m and lag time 0.8 s, the SR sensible heat H_{SR} remained greater than that of eddy covariance H_{EC}. The resulting total evaporation for EC and SR methods were 1.57 mm and 1.10 mm, respectively (Fig. 6.3 (b)). The SR weighting factor (α) determined for this measurement height and lag time (z = 1.2 m and 0.8 s) was 1.01 and the results show an overestimation of H at this height. Thus, the residual calculation of LE_{SR} sometimes resulted in values less than zero, corresponding to condensation, and these values were not used in calculating the daily total evaporation. These results show the sensitivity of SR method to measurement height and lag time with the best results obtained at height 1.2 m above the soil surface and lag of 0.4 s and α value of 1.01 for the cut-grass site. Similar α values found in this study have been reported elsewhere (Mengistu, 2008; Mengistu and Savage, 2010a).

6.3 Conclusions

Sensible heat flux for tall grassland treated by mowing was estimated using the surface renewal (SR) method. Calibration and validation of the SR method was against the eddy covariance (EC) method. The performance of SR method in estimating H was tested at heights of 0.7 and 1.2 m above soil surface using two time lags (0.4 and 0.8 s). The SR weighting factor α for the two heights and time lags was determined, by calibration, indirectly from the slope of the linear regression through the origin of measured H_{EC} values versus H_{SR}. High α values were obtained for fine-wire thermocouple at 0.7 m and time lags 0.4 and 0.8 s ($\alpha = 1.96$ and 2.26, respectively. For a height of 1.2 m and lag times 0.4 and 0.8 s, ($\alpha = 0.71$ and 1.02 were obtained, respectively. LE_{SR} and LE_{EC} calculated as a residual from the shortened energy balance equation gave similar total evaporation estimates. LE_{SR} at different heights (0.7 and 1.2 m) yielded slightly different *ET* estimates due to the sensitivity of the SR method to changing measurement height.

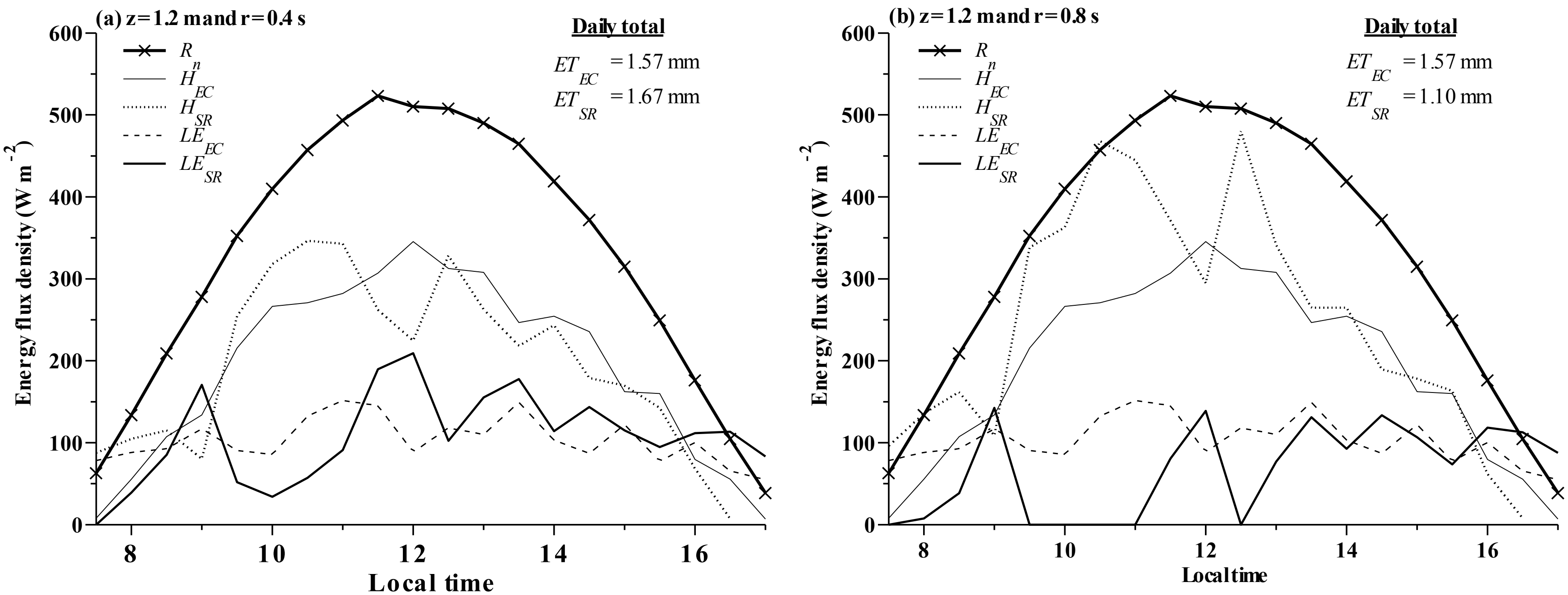

Fig. 6.3 Diurnal variations for day of year 246 (2008) of the half-hourly estimates of H_{EC}, LE_{EC}, H_{SR} and LE_{SR} at a height of 1.2 m above the soil surface at time lags 0.4 and 0.8 s and α value of 1.01.

Chapter 7: Overall conclusions and recommendations for future research

7.1 Overall conclusions

The EC method was successfully tested over naturally occurring tall, mowed and burnt grass surfaces. Radiation and energy balance components were monitored over different grassland surfaces in summer and winter months of 2008 using the EC method and a four-component net radiometer. The tall grassland surface exhibited greater total evaporation (*ET*) in summer than in winter. In the months March to April, *ET* rates ranged from 0.13 to 2.27 mm day^{-1} while *ET* values of 0.25 to 1.28 mm day^{-1} were recorded between May and June (2008). Summer is dominated by greater net irradiance and rainfall distribution resulting in increased soil evaporation and plant transpiration rates. There was a noticeable pattern to the energy balance components observed at the beginning of the experiment at the tall-grassland site. For example, $R_n >> H_{EC} >> G$, was observed from March to June. However, most of the components showed a relative decrease as winter started.

The influence of mowing on the energy balance of a grassland surface was investigated by mowing the tall grass at the cut-grass site to a height of 0.1 m above soil surface. The cut-grass site measurements were compared to the adjacent site that remained undisturbed. Soil temperature was greater for the cut-grass site than the tall-grass site. A diurnal soil temperature range of 12.9 to 18.3 ^{o}C and 13.9 to 21.1 ^{o}C was observed for the tall and cut-grass sites for

DOY 143 to 145 (May) 2008, respectively. It was likely that the differences in temperature regimes for the two sites were due to the differences in the amount of basal cover. For example, the tall-grass site had more cover which may have played a role in reducing the incoming solar irradiance transmitted to the soil surface. This may have led to lower temperatures observed at this site. Both sites showed little variation in soil water content. The cut-grass site had most of its transpiring surface area reduced by mowing, reducing the total evaporation rates observed. Similarly, the tall-grass site had low *ET* rates as the grass stands were dry and not actively growing during winter. Nevertheless, cutting the grass increased its productivity as shoots started to grow faster than plants at the tall-grass site and its *ET* rate was observed to increase as well.

The burning of the tall-grass site caused significant changes to soil water content, soil temperature regimes and surface reflection coefficient. Burning removed most of the litter and this led to a decrease in the surface reflection coefficient of the burnt surface. The burn left the soil bare and the surface was characterized by high temperatures as solar irradiance interception at the soil surface was minimized by lack of litter or mulch and the blackened surface. Similarly, the energy balance components (R_n, H_{EC} and G) also increased following burning. Although the burning event lasted for few minutes, a drastic decrease in soil water content was observed. All changes to grassland surface properties discussed here were gradually reversed after the onset of the spring rains in September, 54 days after the burn. Plants at the burnt grassland site started to develop leaves that eventually covered most of the bare surface. The total evaporation and energy balance components also increased as the burnt grass rejuvenated. The various changes to grassland surface properties collectively contribute to the perturbations to the hydrological cycle. As a result, long-term measurement and monitoring of the energy balance of grasslands subjected to various management practices is crucial especially in relation to climate change and global water budget studies.

A short-term SR analysis was performed above a mixed species and homogeneous tall grassland treated by mowing. The SR method, based on two air temperature structure functions, was calibrated and validated against the EC method using different data sets for unstable conditions during 2008. The SR weighting factor α was determined for two different heights and time lags 0.4 and 0.8 s. High α values were obtained for height 0.7 m and time lags 0.4 and 0.8 s (α = 1.96 and 2.26, respectively) as compared to height 1.2 m and time lags 0.4 and 0.8 s (α = 0.71 and 1.01, respectively). For the validation data set, the SR sensible heat fluxes H_{SR} corresponded reasonably with the EC sensible heat fluxes H_{EC} for height 1.2 m above the soil surface for the 0.4 s lag time.

The total evaporation *ET* for SR method was compared against the EC method, the SR method at measurement height (z) of 1.2 m and time lag of 0.4 s, yielded 1.67 mm while the EC method yielded 1.57 mm for day of year 246 (2008). Conversely, at a measurement height 1.2 m and lag time of 0.8 s, SR and EC methods yielded 1.57 and 1.10 mm, respectively. It is clear that for a lag time of 0.8 s, the SR method overestimated *H* fluxes resulting in very low *LE* calculations. A lag time of 0.4 s is recommended as it resulted in *ET* overestimated by only 0.10 mm compared to an underestimation of 0.47 mm for the 0.8 s time lag.

In this study, both EC and SR methods provided reasonable sensible heat fluxes that compared well at chosen SR measurement heights and time lags. As a result, total evaporation *ET* was estimated as a residual accurately provided other energy balance components are measured correctly. The mowing and burning experiments may yield valuable information on the surface radiation and energy balance of grasslands exposed to various management practices. Compared to the EC method, the SR method is easy in terms of set up, application and use and much less expensive. However, the SR method does require calibration and validation against a standard method such as the EC method.

7.2 Recommendations for future research

The use of eddy covariance (EC) and surface renewal (SR) methods gave useful insights on the influence of grassland management practices on the grassland surface radiation and energy balances. Seasonal and diurnal variations of various energy balance components were successfully measured for mowed, burnt and undisturbed grassland surfaces. Information on energy balance fluxes and water loss above various surfaces is important especially in a water-scarce country like South Africa. As a result, the research results of the study will add valuable information (fluxes and evaporation rates above different grass surfaces) for model validation, decision making processes and water resources management.

Future research could repeat the study on different grass surfaces on a larger scale for different climates. This will mean employing methods such as remote sensing and scintillometry even though they are expensive. However, eddy covariance and scintillometry can still be applied for validation of remotely sensed data. Nevertheless, where capital is limited, SR method may be used to repeat the study on a large scale since it can be replicated with minimal cost. Natural and cultivated grasslands within the South African context are exposed to both communal and commercial animal grazing hence it is recommended that similar investigations be conducted to study the influence of grazing on their surface radiation and energy balances.

Grasslands cover about 40% of the Earth's surface and may play a major role in carbon sequestration and release, and hence climate change. Escalating atmospheric CO_2 concentration due to natural and anthropogenic activities and the potential implications on global warming and climate change emphasize the need for future investigations on grassland micrometeorology to include CO_2 concentration monitoring.

References

Abraha, M.G., 2010. Sensible heat flux and evaporation for sparse vegetation using temperature-variance and a dual-source model. PhD thesis, University of KwaZulu-Natal, Pietermaritzburg, South Africa, 217 pp.

Adema, E.O., Buschiazzo, D.E., Babinec, F.J., Rucci, T.E., Hermida, V.F.G., 2004. Mechanical control of shrubs in a semiarid region of Argentina and its effect on soil water content and grassland productivity. Agricultural Water Management 68, 185-194.

Allen, R.G., Pereira, L.S., Raes, D., Smith, M., 1998. Crop evapotranspiration: Guidelines for computing crop water requirements, FAO Irrigation and Drainage paper 56. Food and Agriculture Organisation of the United Nations, Rome, Italy, 315 pp.

Angle, R.P., Brennand, M., Sandhu, H.S., 1992. Surface albedo measurements at 53^{o}N latitude. Atmospheric Environment. Part A. General Topics 26, 1545-1547.

Antonia, R.A., Chambers, A.J., Bradley, E.F., 1982. Relationships between structure functions and temperature ramps in the atmospheric surface layer. Boundary-Layer Meteorology 23, 395-403.

Arya, S.P., 1988. Introduction to Micrometeorology. Academic Press. London, UK, 307 pp.

Baldocchi, D.D., Xu, L., Kiang, N., 2004. How plant functional-type, weather, seasonal drought, and soil physical properties alter water and energy fluxes of an oak-grass savanna and an annual grassland. Agricultural and Forest Meteorology 123, 13-19.

Boeken, B., Orenstein, D., 2001. The effect of plant litter on ecosystem properties in a Mediterranean semi-arid shrubland. Journal of Vegetation Science 12, 825-832.

Bremer, D.J., Ham, J.M., 1999. Effect of spring burning on the surface energy balance in a tall grass prairie. Agricultural and Forest Meteorology 97, 43-54.

Bremer, D.J., Ham, J.M., 2010. Net carbon fluxes over burned and unburned native tallgrass prairie. Rangeland Ecology and Management 63, 72-81.

Campbell, G.S., Diak, G.R., 2005. Net and thermal radiation estimation and measurement. In: Hatfield, J.L., Baker, J.M. (Eds), Micrometeorology in Agricultural Systems. Agronomy Monograph no. 47, ASA, CSSA, SSSA Publishers. Madison, Wisconsin, USA, pp. 59-92.

Castellví, F., Martínez-Cob, A., Pérez-Coveta, O., 2006. Estimating sensible and latent heat fluxes over rice using surface renewal. Agricultural and Forest Meteorology 139, 164-169.

Castellví, F., Snyder, R.L., 2010. A comparison between latent heat fluxes over grass using a weighing lysimeter and surface renewal analysis. Journal of Hydrology 381, 213-220.

Castellví, F., Snyder, R.L., Baldocchi, D.D., 2008. Surface energy-balance closure over rangeland grass using the eddy covariance method and surface renewal analysis. Agricultural and Forest Meteorology 148, 1147-1160.

Department of Environmental Affairs and Tourism., 2006. South Africa Environment Outlook. A report on the state of the environment. Department of Environmental Affairs and Tourism, Pretoria, 370 pp.

Dillon, R.F., 1980. Some effects of fire in the tall grassveld of Natal. MSc thesis, University of Natal, Pietermaritzburg, South Africa, 132 pp.

Dye, P.Y., Olbrich, B.W., Poulter, A.G., 1991. The influence of growth rings in *Pinus patula* on heat pulse velocity and sapflow measurement. Journal of Experimental Botany 42, 867-870.

Edwards, P.J., 1984. The use of fire as a management tool. In: Booysen, P.d.V, Tainton, N.M. (Eds), Ecological Effects of Fire in South African Ecosystems. Springer-Verlag. Berlin, Germany, pp. 349-362.

Edwards, P.J., Tainton, N.M., 1990. Managed grasslands in South Africa. In: Breymeyer, A.I. (Eds), Managed Grasslands: Regional Studies. Elsevier. Amsterdam, Netherlands, pp. 99-128.

Edwards, W.R.N., Warwick, N.W.M., 1984. Transpiration from a kiwifruit vine as estimated by the heat pulse technique and the Penman-Monteith equation. New Zealand Journal of Agricultural Research 27, 537-543.

Emmerich, W.E., 2007. Ecosystem water use efficiency in a semiarid shrubland and grassland community. Rangeland Ecology and Management 60, 464-470.

Everson, C.S., 2001. The water balance of a first order catchment in the montane grasslands of South Africa. Journal of Hydrology 241, 110-123.

Everson, C.S., Molefe, G.L., Everson, T.M., 1998. Monitoring and modelling components of the water balance in a grassland catchment in the summer rainfall area of South Africa. Water Research Commission Report No. 493/1/98, p138, Pretoria, South Africa. ISBN 1-86845-443-6.

Falge, E., Reth, S., Brüggemann, N., Butterbach-Bahl, K., Goldberg, V., Oltchev, A., Schaaf, F., Spindler, G., Stiller, B., Queck., R., Köstner, B., Berhofer, C., 2005. Comparison of surface energy exchange models with eddy flux data in forest and grassland ecosystems of Germany. Agricultural and Forest Meteorology 188, 174-216.

Falkenmark, M., 1989. The massive water scarcity now threatening Africa: Why isn't it being addressed? Ambio 18, 112-118.

Falkenmark, M., 1990. Rapid population growth and water scarcity: The predicament of tomorrow's Africa. Population and Development Review 16, 81-94.

Finnigan, J.J., 2004. A re-evaluation of long-term flux measurement techniques Part II: Coordinate systems. Boundary-Layer Meteorology 113, 1-41.

Fritschen, L.J., Gay, L.W., 1979. Environmental Instrumentation. Springer-Verlag. New York, USA, 216 pp.

Fynn, R.W.S., Morris, C.D., Edwards, T.J., 2004. Effect of burning and mowing on grass and forb diversity in a long-term grassland experiment. Applied Vegetation Science 7, 1-10.

Gasca-Tucker, D.L., Acreman, M.C., Agnew, C.T., Thompson, J.R., 2007. Estimating evaporation from a wet grassland. Hydrology and Earth System Sciences 11, 270-282.

Gavin, H., Agnew, C.T., 2000. Estimating evaporation and surface resistance from a wet grassland. Physics and Chemistry of the Earth, Part B: Hydrology, Oceans and Atmosphere 25, 599-603.

Graversen, R., Wang, M., 2009. Polar amplification in a coupled climate Model with locked albedo. Climate Dynamics 33, 629-643.

Grebet, P., Cuenca, R.H., 1991. History of lysimeter design and effects of environmental disturbances. In: Allen, R.G., Howell, T.A., Pruitt, W.O., Walter, I.A., Jensen, M.E. (Eds), Lysimeters for Evapotranspiration and Environmental Measurements. Proceedings of the International Symposium on Lysimetry, July 23-25, 1991, ASCE Publication, Honolulu, Hawaii, pp. 10-18.

Hall, R.L., Allen, S.J., Rosier, P.T.W., Hopkins, R., 1998. Transpiration from coppiced poplar and willow measured using sap-flow methods. Agricultural and Forest Meteorology 90, 275-290.

Harrington, G.N., Wilson, A.D., Young, M.D., 1984. Management of rangeland ecosystems. In: Harrington, G.N., Wilson, A.D., Young, M.D. (Eds), Management of Australia's Rangelands. Commonwealth Scientific and Industrial Research Organisation. Melbourne, Australia, pp. 3-14.

Hellmann, D.B., 1976. The study of water use in wheat in relation to environment and yield, on the Makatini Flats, using lysimeters and neutron probe. MSc thesis, University of Natal, Pietermaritzburg, South Africa, 205 pp.

Hill, R.J., 1992. Review of optical scintillation methods of measuring the refractive-index spectrum, inner scale and surface fluxes. Waves in Random Media 2, 179-201.

Hodgkinson, K.C., Harrington, G.N., Griffin, G.F., Noble, J.C., Young, M.D., 1984. Management of vegetation with fire. In: Harrington, G.N., Wilson, A.D., Young, M.D. (Eds), Management of Australia's Rangelands. Commonwealth Scientific and Industrial Research Organisation. Melbourne, Australia, pp. 141-156.

Horst, T.W., Weil, J.C., 1994. How far is far enough?: The fetch requirements for micrometeorological measurement of surface fluxes. Journal of Atmospheric and Oceanic Technology 11, 1018-1025.

Howell, T.A., Schneider, A.D., Jensen, M.E., 1991. History of lysimeter design and use for evapotranspiration measurements. In: Allen, R.G., Howell, T.A., Pruitt, W.O., Walter, I.A., Jensen, M.E. Lysimeters for evapotranspiration and environmental measurements. Proceedings of the International Symposium on Lysimetry, July 23-25, 1991, ASCE Publication, Honolulu, Hawaii, pp. 1-9.

Hunt, J.E., Kelliher, F.M., McSeveny, T.M., Byers, J.N., 2002. Evaporation and carbon dioxide exchange between the atmosphere and a tussock grassland during a summer drought. Agricultural and Forest Meteorology 111, 65-82.

Hurtalová, T., Matejka, F., 1999. Surface characteristics and energy fluxes above different plant canopies. Agricultural and Forest Meteorology 98, 491-500.

Idso, S.B., 1976. Complexities of surface albedo determinations during duststorms. Atmospheric Environment 10, 5-7.

Inoue, J., Hori, M.E., 2011. Arctic cyclogenesis at the marginal ice zone: a contributory mechanism for the temperature amplification? Geophysical Research Letters 38, LI2502, 1-6.

Jacobs, A.F.G., Heusinkveld, B.G., Holtslag, A.A.M., 2008. Towards closing the surface energy balance of a mid-latitude grassland. Boundary-Layer Meteorology 126, 125-136.

Jarmain, C., 2003. Potential for using trees to limit the ingress of water into the mine workings: A comparison of total evaporation and soil water relations for *Eucalyptus* and grassland. PhD thesis, University of Natal, Pietermaritzburg, South Africa, 219 pp.

Klassen, S., Bugbee, B., 2005. Shortwave radiation. In: Hatfield, J.L., Baker, J.M. (Eds), Micrometeorology in Agricultural Systems. Agronomy Monograph no. 47, ASA, CSSA, SSSA Publishers. Madison, Wisconsin, USA, pp. 43-57.

Köstner, B., Granier, A., Cermák, J., 1998. Sapflow measurements in forest stands: Methods and uncertainties. Annals of Forest Science 55, 13-27.

Limb, R.F., Fuhlendorf, S.D., Engle, D.M., Kerby, J.D., 2011. Growing-season disturbance in tallgrass prairie: Evaluating fire and grazing on *Schizachyrium scoparium*. Rangeland Ecology and Management 64, 28-36.

Liou, K.N., 2002. An Introduction to Atmospheric Radiation. Second Edition. Academic Press. London, UK, 583 pp.

Mauder, M., Oncley, S., Vogt, R., Weidinger, T., Ribeiro, L., Bernhofer, C., Foken, T., Kohsiek, W., de Bruin, H., Liu, H., 2007. The energy balance experiment EBEX-2000. Part II: Intercomparison of eddy-covariance sensors and post-field data processing methods. Boundary-Layer Meteorology 123, 29-54.

Mengistu, M.G., 2008. Heat and energy exchange above different surfaces using surface renewal. PhD thesis, University of KwaZulu-Natal, Pietermaritzburg, South Africa, 151 pp.

Mengistu, M.G., Savage, M.J., 2010a. Surface renewal method for estimating sensible heat flux. Water SA 36, 9-17.

Mengistu, M.G., Savage, M.J., 2010b. Open water evaporation estimation for a small shallow reservoir in winter using surface renewal. Journal of Hydrology 380, 27-35.

Moran, M.S., Scott, R.L., Keefer, T.O., Emmerich, W.E., Hernandez, M., Nearing, G.S., Paige, G.B., Cosh, M.H., O'Neill, P.E., 2009. Partitioning evapotranspiration in semiarid grassland and shrubland ecosystems using time series of soil temperature. Agricultural and Forest Meteorology 149, 59-72.

Mottram, R., 1976. Measurement of evapotranspiration from *Lolium multiflorun* and *Paspalum dilatatum* and its dependence upon the climatic variables. MSc thesis, University of Natal, Pietermaritzburg, South Africa, 93 pp.

Nakai, T., van der Molen, M.K., Gash, J.H.C., Kodama, Y., 2006. Correction of sonic anemometer angle of attack errors. Agricultural and Forest Meteorology 136, 19-30.

Nile, E.S., 2010. Sensible heat flux estimation under unstable conditions for sugarcane using temperature variance and surface renewal. PhD thesis, University of KwaZulu-Natal, Pietermaritzburg, South Africa, 171 pp.

Novak, M.D., 2005. Soil temperature. In: Hatfield, J.L., Baker, J.M. (Eds), Micrometeorology in Agricultural Systems. Agronomy Monograph no. 47, ASA, CSSA, SSSA Publishers. Madison, Wisconsin, USA, pp. 105-129.

Novick, K.A., Stoy, P.C., Katul, G.G., Ellsworth, D.S., Siqueira, M.B.S., Juang, J., Oren, R., 2004. Carbon dioxide and water vapor exchange in a warm temperate grassland. Oecologia 138, 259-274.

Odhiambo, G.O., 2007. Long-term measurements of spatially-averaged sensible heat flux for a mixed grassland community, using surface layer scintillometry. PhD thesis, University of KwaZulu-Natal, Pietermaritzburg, South Africa, 151 pp.

Odhiambo, G.O., Savage, M.J., 2009. Surface layer scintillometry for estimating the sensible heat flux component of the surface energy balance. South African Journal of Science 105, 208-216.

Oluwole, F.A., Sambo, J.M., Schalazo, D., 2008. Long-term effects of different burning frequencies on the dry savannah grassland in South Africa. African Journal of Agricultural Research 3, 147-153.

Orlando, S., Bale, A., Johnson, D.A., 2011. Experimental study of the effect of tower shadow on anemometer readings. Journal of Wind Engineering and Industrial Aerodynamics 99, 1-6.

Paw U, K.T., Qui, J., Su, H.B., Watanabe, T., Brunet, Y., 1995. Surface renewal analysis: a new method to obtain scalar fluxes. Agricultural and Forest Meteorology 74, 119-137.

Paw U, K.T., Snyder, R.I., Spano, D., Su, H.B., 2005. Surface renewal estimates of scalar exchange. In: Hatfield, J.L., Baker, J.M. (Eds), Micrometeorology in Agricultural Systems. Agronomy Monograph no. 47, ASA, CSSA, SSSA Publishers. Madison, Wisconsin, USA, pp. 455-485.

Pearson, C.J., Ison, R.L., 1997. Agronomy of Grassland Systems. Second Edition. Cambridge University Press. Cambridge, United Kingdom, 222 pp.

Penman, H.L., 1948. Natural evaporation from open water, bare soil and grass. Proceedings of the Royal Society of London. Series A, Mathematical and Physical Sciences 193, 120-145.

Postel, S.L., 2000. Entering an era of water scarcity: The challenges ahead. Ecological Applications 10, 941-948.

Richiardone, R., Giampiccolo, E., Ferrarese, S., Manfrin, M., 2008. Detection of flow distortions and systematic errors in sonic anemometry using the planar fit method. Boundary-Layer Meteorology 128, 277-302.

Rose, C.W., 1966. Agricultural Physics. Pergamon Press. London, Edinburgh, 256 pp.

Rosset, M., Riedo, M., Grub, A., Geissmann, M. and Fuhrer, J., 1997. Seasonal variation in Radiation and energy balances of permanent pastures at different altitudes. Agricultural and Forest Meteorology 86, 245-258.

Sakuratani, T., 1981. A heat balance method for measuring water flux in the stem of intact plants. Journal of Agricultural Meteorology 37, 9-17.

Sanderson, M.A., 2008. Upland switchgrass yield, nutritive value, and soil carbon changes under grazing and clipping. Agronomy Journal 100, 510-516.

Sauer, T.J., Horton, R., 2005. Soil heat flux. In: Hatfield, J.L., Baker, J.M. (Eds), Micrometeorology in Agricultural Systems. Agronomy Monograph no. 47, ASA, CSSA, SSSA Publishers. Madison, Wisconsin, USA, pp. 131-154.

Savage, M.J., 1980. The effect of fire on the grassland microclimate. Herbage Abstracts 50, 589-603.

Savage, M.J., 2009. Estimation of evaporation using a dual-beam surface layer scintillometer and component energy balance measurements. Agricultural and Forest Meteorology 149, 501-517.

Savage, M.J., 2010a. Field evaluation of polymer capacitive humidity sensors for Bowen ratio energy balance flux measurements. Sensors 10, 7748-7771.

Savage, M.J., 2010b. Sensible heat flux for estimating evaporation. DScAgric thesis, University of KwaZulu-Natal, Pietermaritzburg, South Africa, 343 pp.

Savage, M.J., Everson, C.S., Graham, A.D.N., Lightbody, K.E., 2000. An investigation of the stem steady state heat energy balance technique in determining water use by trees. Water Research Commission Report No. 348/1/00, 181 pp, Pretoria, South Africa. ISBN 1-86845-617-X.

Savage, M.J., Everson, C.S., Metelerkamp, B.R., 1997. Evaporation measurement above vegetated surfaces using micrometeorological techniques. Water Research Commission Report No. 349/1/97, 226 pp, Pretoria, South Africa. ISBN 1-86845-363-4.

Savage, M.J., Everson, C.S., Metelerkamp, B.R., 2009. Bowen ratio evaporation measurement in a remote montane grassland: Data integrity and fluxes. Journal of Hydrology 376, 249-260.

Savage, M.J., Everson, C.S., Odhiambo, G.O., Mengistu, M.G., Jarmain, C., 2004. Theory and practice of evapotranspiration measurement, with special focus on SLS as an operational tool for the estimation of spatially-averaged evaporation. Water Research Commission Report No. 1335/1/04, 204 pp, Pretoria, South Africa. ISBN 1-77005-247-X.

Savage, M.J., Odhiambo, G.O., Mengistu, M.G., Everson, C.S., Jarmain, C., 2010. Measurement of grassland evaporation using a surface-layer scintillometer. Water SA 36, 1-8.

Savage, M.J., Vermeulen, K., 1983. Microclimate modification of tall moist grasslands of Natal by spring burning. Journal of Range Management 36, 172-174.

Serreze, M.C., Barrett, A.P., Stroeve, J.C., Kindig, D.N., Holland, M.M., 2009. The emergence of surface-based Arctic amplification. The Cryosphere 3, 11-19.

Smith, D.M. and Allen, S.J., 1996. Measurement of sap flow in plant stems. Journal of Experimental Botany 47, 1833-1844.

Snyder, R.L., Spano, D., Paw U, K.T., 1996. Surface renewal analysis for sensible heat and latent flux density. Boundary-Layer Meteorology 77, 249-266.

Snyman, H.A., 1999. Quantification of the soil-water balance under different veld condition classes in a semi-arid climate. African Journal of Range & Forage Science 16, 108-117.

Sumner, D.M., Jacobs, J.M., 2005. Utility of Penman-Monteith, Priestly-Taylor, reference evapotranspiration, and pan evaporation methods to estimate pasture evapotranspiration. Journal of Hydrology 308, 81-104.

Sun, J., 2007. Tilt corrections over complex terrain and their implication for CO_2 transport. Boundary-Layer Meteorology 124, 143-159.

Twine, T.E., Kustas, W.P., Norman, J.M., Cook, D.R., Houser, P.R., Meyers, T.P., Prueger, J.H., Starks, P.J., Wesely, M.L., 2000. Correcting eddy-covariance flux underestimates over a grassland. Agricultural and Forest Meteorology 103, 279-300.

United Nations., 2009a. World Population Prospects: The 2008 Revision. Department of Economics and Social Affairs, Population Division, New York, USA.

United Nations., 2009b. Water in the changing world. The 3rd United Nations world water development report. UNESCO publishing, Paris, London, UK.

Van Atta, C.W., 1977. Effect of coherent structures on structure functions of temperature in the atmospheric boundary layer. Archives of Mechanics 29, 161-171.

Van Riper, G.E., Owen, F.G., 1964. Effect of cutting height on alfalfa and two grasses as related to production, persistence, and available soil moisture. Agronomy Journal 56, 291-295.

Vermeire, L.T., Webster, D.B., Mitchell, R.B., Fuhlendorf, A.D., 2005. Fire and grazing effects on wind erosion, soil water content, and soil temperature. Journal of Environmental Quality 34, 1559-1565.

Vickers, D., Mahrt, L., 2006. Contrasting mean vertical motion from tilt correction methods and mass continuity. Agricultural and Forest Meteorology 138, 93-103.

Villa Nova, N.A., Pereira, A.B., Shock, C.C., 2007. Estimation of reference evapotranspiration by an energy balance approach. Biosystems Engineering 96, 605-615.

Wang, S., Davidson, A., 2007. Impact of climate variations on surface albedo of a temperate grassland. Agricultural and Forest Meteorology 142, 133-142.

Watts, C.J., Chehbouni, A., Rodriguez, J.-C., Kerr, Y.H., Hartognesis, O., de Bruin, H.A.R., 2000. Comparison of sensible heat flux estimates using AVHRR with scintillometer measurements over semi-arid grassland in northwest Mexico. Agricultural and Forest Meteorology 105, 81-89.

Wever, L.A., Flanagan, L.B., Carlson, P.J., 2002. Seasonal and interannual variation in evapotranspiration, energy balance and surface conductance in a northern temperate grassland. Agricultural and Forest Meteorology 112, 31-49.

Wilczak, J., Oncley, S., Stage, S., 2001. Sonic anemometer tilt correction algorithms. Boundary-Layer Meteorology 99, 127-150.

Wilson, A.D., Tongway. D.J., Graetz, R.D., Young, M.D., 1984. Range inventory and monitoring. In: Harrington, G.H., Wilson, A.D., Young, M.D. (Eds), Management of Australia's Rangelands. Commonwealth Scientific and Industrial Research Organisation. Melbourne, Australia, pp. 113-128.

Wright, H.A., Bailey, A.W., 1982. Fire Ecology: United States and Southern Canada. Wiley-Interscience, New York, 501 pp.

Zapata, N., Martínez-Cob, A., 2002. Evaluation of the surface renewal method to estimate wheat evapotranspiration. Agricultural Water Management 55, 141-151.